2013-12

Effect of Doppler shift on adaptive OFDM modulation for cognitive radio application

Ahn, Byunghyun

Monterey, California: Naval Postgraduate School

NAVAL POSTGRADUATE SCHOOL

MONTEREY, CALIFORNIA

THESIS

EFFECT OF DOPPLER SHIFT ON ADAPTIVE OFDM MODULATION FOR COGNITIVE RADIO APPLICATION

by

Byunghyun Ahn

December 2013

Thesis Advisor: Ric A. Romero
Co-Advisors: Tri T. Ha
Weilian Su

THIS PAGE INTENTIONALLY LEFT BLANK

REPORT DOCUMENTATION PAGE			Form Approved OMB No. 0704–0188

1. AGENCY USE ONLY *(Leave blank)*	2. REPORT DATE December 2013	3. REPORT TYPE AND DATES COVERED Master's Thesis

4. TITLE AND SUBTITLE EFFECT OF DOPPLER SHIFT ON ADAPTIVE OFDM MODULATION FOR COGNITIVE RADIO APPLICATION	5. FUNDING NUMBERS
6. AUTHOR(S) Byunghyun Ahn	
7. PERFORMING ORGANIZATION NAME(S) AND ADDRESS(ES) Naval Postgraduate School Monterey, CA 93943–5000	8. PERFORMING ORGANIZATION REPORT NUMBER
9. SPONSORING /MONITORING AGENCY NAME(S) AND ADDRESS(ES) N/A	10. SPONSORING/MONITORING AGENCY REPORT NUMBER

11. SUPPLEMENTARY NOTES The views expressed in this thesis are those of the author and do not reflect the official policy or position of the Department of Defense or the U.S. Government. IRB Protocol number ____N/A____.

12a. DISTRIBUTION / AVAILABILITY STATEMENT Approved for public release; distribution is unlimited	12b. DISTRIBUTION CODE A

13. ABSTRACT (maximum 200 words)

In this thesis, the effect of Doppler shift on adaptive orthogonal frequency-division multiplex (OFDM) modulation in a cognitive radio (CR) application is investigated. We present Monte Carlo simulations of OFDM modulation in which a group or groups of subcarriers are modulated using quadrature phase-shift keying (QPSK) modulation and 16-ary quadrature amplitude modulations (16QAM). We show that turning off some subcarriers does not affect the performance as long as the effective E_b/N_o remains the same. We also present Monte Carlo simulations where the power ratio of two sets of subcarriers is changed while maintaining the same total power in order to investigate the effect on performance. Finally, we consider a two-user CR scenario and investigate the performance effect on a primary user by a secondary user in terms of various Doppler shift offsets where both the primary user and secondary user use OFDM modulations.

14. SUBJECT TERMS Cognitive Radio (CR), Signal-to-Noise Ratio (SNR), Signal-to-Interference Ratio (SIR), Adaptive Orthogonal Frequency Division Multiplexing (AOFDM), Frequency Offset, Doppler shift, Quadrature Phase Shift Keying (QPSK), Quadrature Amplitude Modulations (QAM), Subcarrier Allocation Scheme	15. NUMBER OF PAGES 77
	16. PRICE CODE

17. SECURITY CLASSIFICATION OF REPORT	18. SECURITY CLASSIFICATION OF THIS PAGE	19. SECURITY CLASSIFICATION OF ABSTRACT	20. LIMITATION OF ABSTRACT
Unclassified	Unclassified	Unclassified	UU

NSN 7540–01–280–5500 Standard Form 298 (Rev. 2–89)
Prescribed by ANSI Std. 239–18

THIS PAGE INTENTIONALLY LEFT BLANK

Approved for public release; distribution is unlimited

EFFECT OF DOPPLER SHIFT ON ADAPTIVE OFDM MODULATION FOR COGNITIVE RADIO APPLICATION

Byunghyun Ahn
Lieutenant, Republic of Korea Navy
B.S., Republic of Korea Naval Academy, 2005

Submitted in partial fulfillment of the
requirements for the degree of

MASTER OF SCIENCE IN ELECTRICAL ENGINEERING

from the

NAVAL POSTGRADUATE SCHOOL
December 2013

Author: Byunghyun Ahn

Approved by: Ric A. Romero
Thesis Advisor

Tri T. Ha
Thesis Co-Advisor

Weilian Su
Thesis Co-Advisor

Ralph C. Robertson
Chair, Department of Electrical and Computer Engineering

THIS PAGE INTENTIONALLY LEFT BLANK

ABSTRACT

In this thesis, the effect of Doppler shift on adaptive orthogonal frequency-division multiplex (OFDM) modulation in a cognitive radio (CR) application is investigated. We present Monte Carlo simulations of OFDM modulation in which a group or groups of subcarriers are modulated using quadrature phase-shift keying (QPSK) modulation and 16-ary quadrature amplitude modulations (16QAM). We show that turning off some subcarriers does not affect the performance as long as the effective E_b/N_o remains the same. We also present Monte Carlo simulations where the power ratio of two sets of subcarriers is changed while maintaining the same total power in order to investigate the effect on performance. Finally, we consider a two-user CR scenario and investigate the performance effect on a primary user by a secondary user in terms of various Doppler shift offsets where both the primary user and secondary user use OFDM modulations.

THIS PAGE INTENTIONALLY LEFT BLANK

TABLE OF CONTENTS

THIS PAGE INTENTIONALLY LEFT BLANK

LIST OF FIGURES

THIS PAGE INTENTIONALLY LEFT BLANK

LIST OF TABLES

THIS PAGE INTENTIONALLY LEFT BLANK

LIST OF ACRONYMS AND ABBREVIATIONS

16QAM	16-ary Quadrature Amplitude Modulation
BER	Bit Error Ratio
CR	Cognitive Radio
FCC	Federal Communications Commission
FFT	Fast Fourier Transform
ICI	Inter Carrier Interference
OFDM	Orthogonal Frequency-Division Multiplexing
PSD	Power Spectral Density
PU	Primary User
QPSK	Quadrature Phase-Shift Keying
Rx	Receivers
SER	Symbol Error Ratio
SIR	Signal-to-Interference ratio
SNR	Signal-to-Noise Ratio
SU	Secondary User
Tx	Transmitters

THIS PAGE INTENTIONALLY LEFT BLANK

EXECUTIVE SUMMARY

In this thesis, a cognitive radio (CR) application is investigated in terms of Doppler shift on adaptive orthogonal frequency-division multiplex (OFDM) modulation. Adaptive OFDM may be used in CR where the secondary users (SU) are allowed to use frequency bands allocated to the primary users (PU) that are not in use. Thus, for OFDM to work for a SU, there is a need to turn off subcarriers in frequency bands that are used by PU. We present simulated spectra in the frequency domain where some carriers are clearly used and others are turned off. With the use of Monte Carlo simulations using Matlab, we are able to show bit error ratio (BER) and symbol error ratio (SER) performance curves for some scenarios where subcarriers are turned off and compare them to theoretical BER and SER expressions as a function of increasing signal-to-noise ratio (***SNR***). In Table 1, we show the utilization of the subcarriers in one of our simulation scenarios. We use quadrature phase-shift keying (QPSK) modulation with OFDM where the first four and third subcarriers are used and the second and last four subcarriers are turned off. The BER and SER for this scenario (4 ON, 4 OFF, 4 ON and 4 OFF subcarriers with QPSK-OFDM) are shown in Figure 1. We observe that the BER and SER resulting from Monte Carlo simulation are in good agreement with the theoretical bit error ratio and symbol error ratio for QPSK modulation. In this thesis, we also consider a few more scenarios in which there are eight subcarriers (4 ON, 4 OFF), 12 subcarriers (4 ON, 4 OFF, 4 ON) and 16 subcarriers (4 ON, 4 OFF, 4 ON, 4 OFF) with QPSK and 16QAM (16-ary quadrature amplitude modulation). The results of these scenarios show that the BER and SER for each scenario are in good agreement with theoretical BER and SER for QPSK or 16QAM.

Table 1. Subcarrier utilization of 16 subcarrier OFDM: first four and third four subcarriers are used for QPSK and the second four and last four subcarriers are turned off.

SC 1~4	SC 5~8	SC 9~12	SC 13~16
QPSK Symbols	OFF	QPSK Symbols	OFF

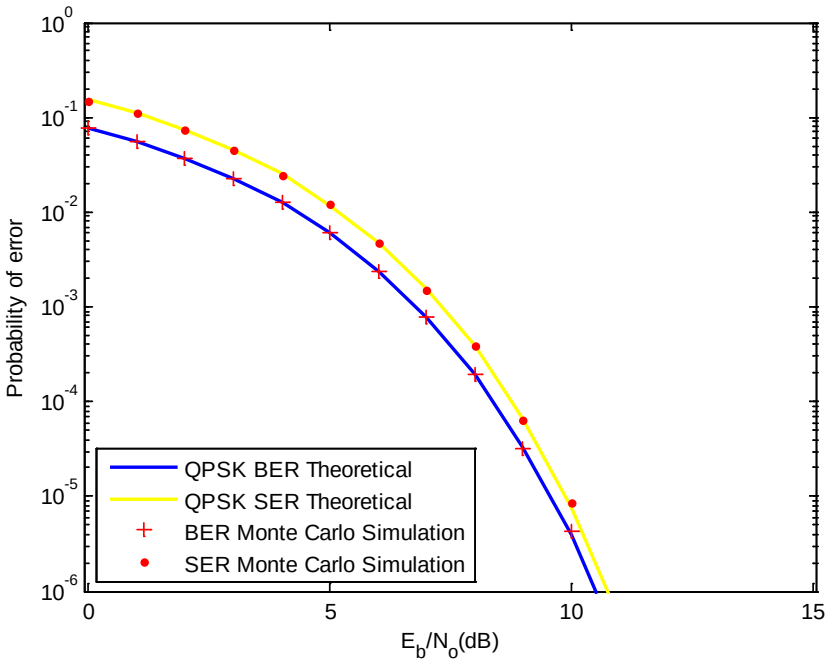

Figure 1. Performance curves for the 16 subcarrier (4 ON, 4 OFF, 4 ON, 4 OFF, QPSK-OFDM) scenario vs. E_b/N_o.

In this work, we also consider changing the power ratio for a specific 12-subcarrier scenario (4 ON, 4 OFF, 4 ON). We allow for the first and last four subcarriers to be used. In this scenario, we adjust the average power ratio between the first four subcarriers and last four subcarriers, while the sum of total subcarrier power does not change. Recall the middle four subcarriers are turned off. In other words, the set of channels in the middle is not used, and the two bands that are used have different power. The performance curves from the simulations in which we use QPSK as a modulation scheme in the utilized bands are shown in Figure 2. The power ratio 1:1 results in the best performance, which means equal power allocation is best when the number of subcarriers in the bands that are available is equal. In other words, as we increase the power ratio between two subcarriers sets, the performance becomes worse. The conclusion of this simulation is that equal power allocation is best for OFDM using the same modulation and equal number of subcarriers (when two or more bands are available for use).

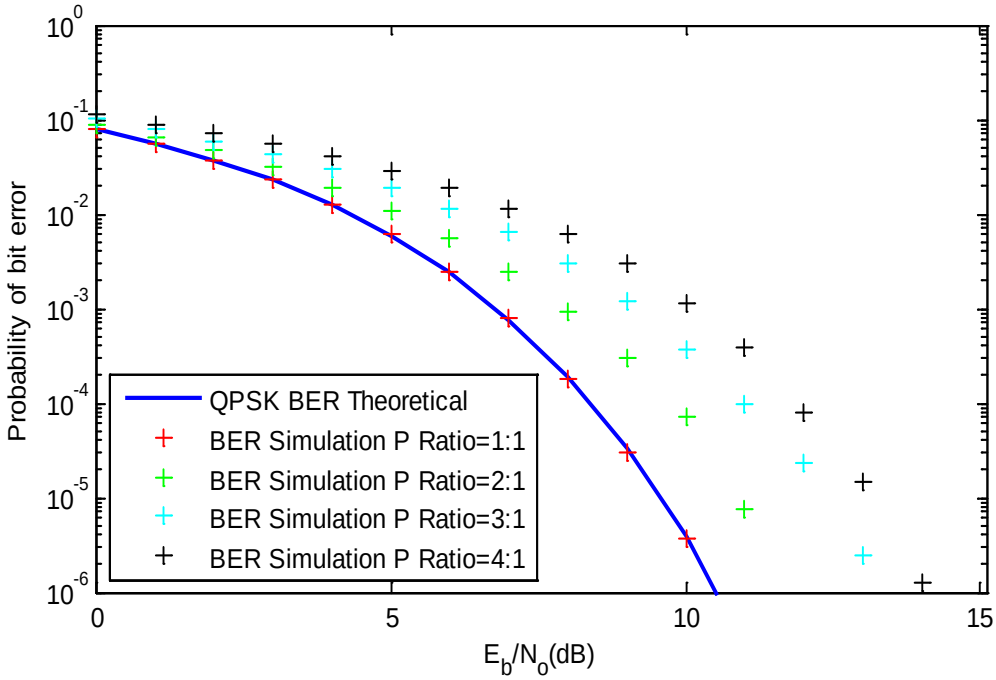

(a)

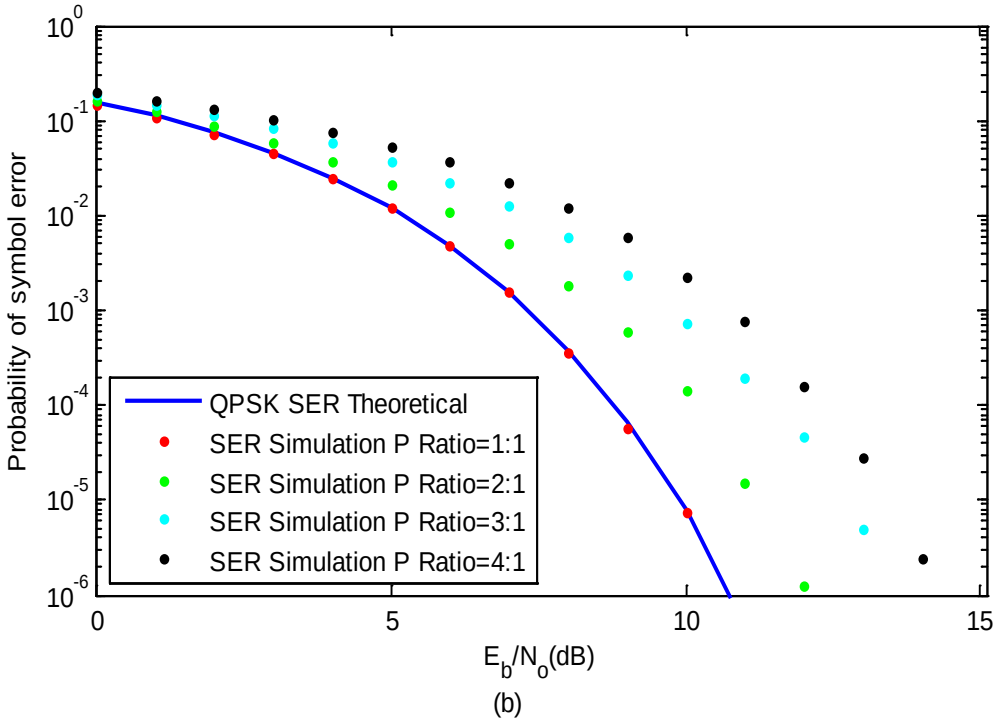

(b)

Figure 2. Performance curves for the 12 subcarrier (4 ON, 4 OFF, 4 ON, QPSK-OFDM) scenario vs. E_b/N_o. as a function of power ratio: (a) BER; (b) SER.

The last topic we considered was a two-user cognitive radio scenario. In Figure 3, PU (primary user) and SU (secondary user) transmitters (TX) and receivers (Rx) are shown. In this scenario the SU's signal can act as interference to the PU. In this simulation set, we investigate the effect on PU performance by varying Doppler shifts to the SU spectrum. In addition, we also vary the PU-to-SU power ratio, which equivalently is the signal-to-interference power ratio (***SIR***) while varying the Doppler offset. We use 16 subcarriers (4 ON, 4 OFF, 4 ON, 4 OFF) for PU (4 OFF, 4 ON, 4 OFF, 4 OFF) for SU. In other words, the SU uses one of the empty channels. With these settings we generate the PU's BER and SER for changing ***SIR*** and the percentage of frequency offset.

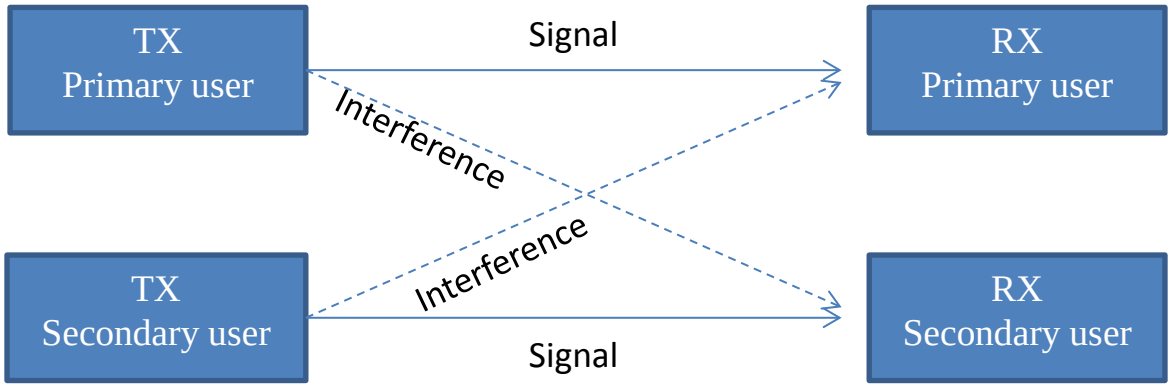

Figure 3. Concept diagram of transmission and reception in a two-user CR where Doppler shifts may result in interferences.

One of the BER/SER set for the PU as a function of Doppler shift when ***SIR***=0 is shown in Figure 4. The results show that without frequency offset, the performance of SU is in good agreement with the QPSK theoretical BER/SER curve. With frequency offset, as the frequency offset is increased, the BER/SER of PU becomes worse. As we increase ***SIR*** while holding the frequency offset fixed, we observe improved BER/SER for the PU. We conclude that the larger frequency offset of the SU results in worse performance for the PU, and the larger PU receiver ***SIR*** while holding the Doppler constant results in better performance as expected.

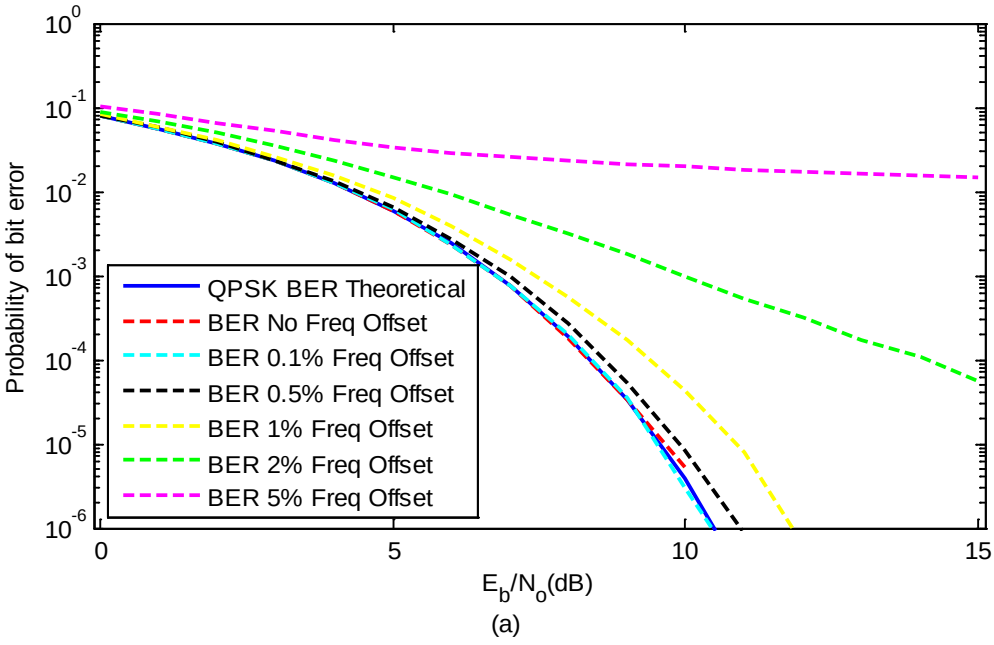

(a)

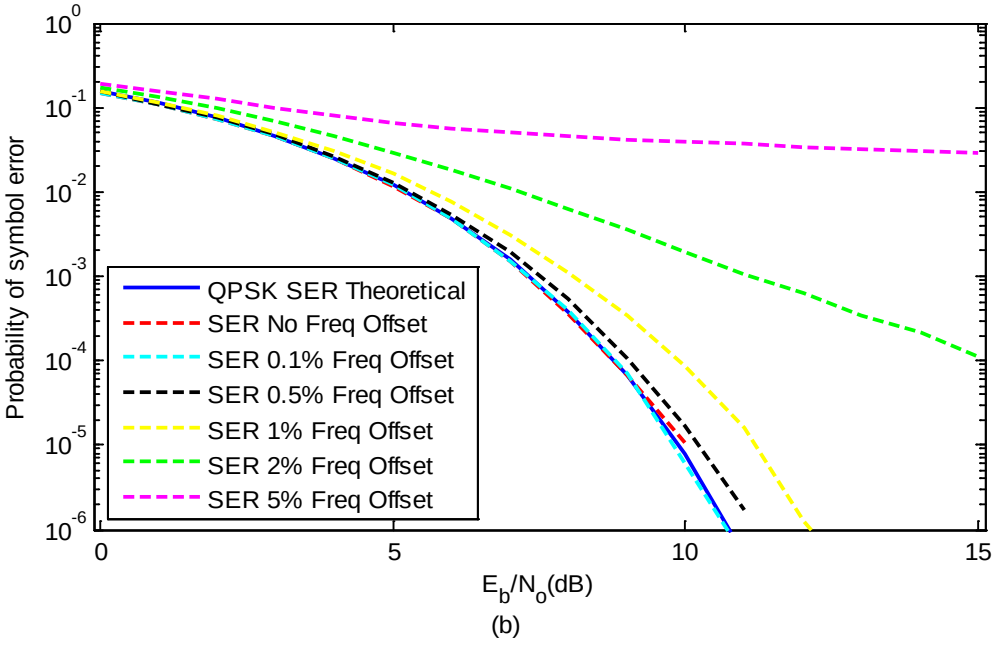

(b)

Figure 4. BER performance of PU as a function of Doppler shift on SU where the % frequency offset is the percent over the PU available bandwidth: (a) BER at ***SIR*** = 0 dB; (b) SER at ***SIR*** = 0 dB.

THIS PAGE INTENTIONALLY LEFT BLANK

ACKNOWLEDGMENTS

I would like to express my sincere gratitude to my advisor Professor Ric A. Romero, for continuous support of my research, for his patience, motivation and enthusiasm. His guidance helped me through the thorny times in my research, and helped me move forward when I felt truly lost. I could not have imagined having a better advisor and mentor.

I would like to thank my co-advisors: Dr. Tri T. Ha and Professor Weilian Su for their advice, engagement, and insightful comments that were invaluable to my success here.

I also would like to specially thank Matthew Porter for his moral encouragement during this process. I could not have endured my school life without the steadfast support he supplied.

Last, but certainly not least, I want to thank my wife, Huijeong, and daughter, Joy, for their love and encouragement during my studies here. I would not have been able to devote the long hours without their support.

THIS PAGE INTENTIONALLY LEFT BLANK

I. INTRODUCTION

A. OVERVIEW

The demand for radio spectrum has been increasing rapidly as wireless communications such as audio, messaging, and Internet access via smartphones become widespread. Wireless communication devices usually transmit and receive large amounts of multimedia data like music, pictures and movies that require high data rates in a network and, thus, use much of the spectrum resources. So, it is important for a system to use the radio spectrum efficiently within the limited bandwidth resources. Spectrum efficiency means transmitting and receiving as much data as possible within the available spectrum. A study from the Federal Communications Commission (FCC) reported that physical shortage of spectrum is not the issue; rather it is the efficient use of the spectrum. So the FCC recommends a flexible spectrum regulation policy [1]. To solve the spectrum availability issue, communication technology is being developed for multiusers in a way that the radio spectrum is used efficiently.

1. Subcarrier Allocation Scheme over OFDM

Orthogonal frequency-division multiplexing (OFDM) is a good fit for broadband wireless systems because it has the potential for high transmission efficiency and is less vulnerable to inter-symbol interference. Due to its flexibility in allocating subcarriers, it is adequate for multiuser communication systems. The multiuser allocation system diagram is shown in Figure 1. We assume the system shown has K users, and each k_{th} user has equal data rate R_{k}. In the figure, channel state information is assumed a priori. The subcarrier and bit allocation blocks are used to allocate bits. The combined sub-carrier bit and power allocation algorithm blocks are used to adjust the number of bits/OFDM symbol on each subcarrier.

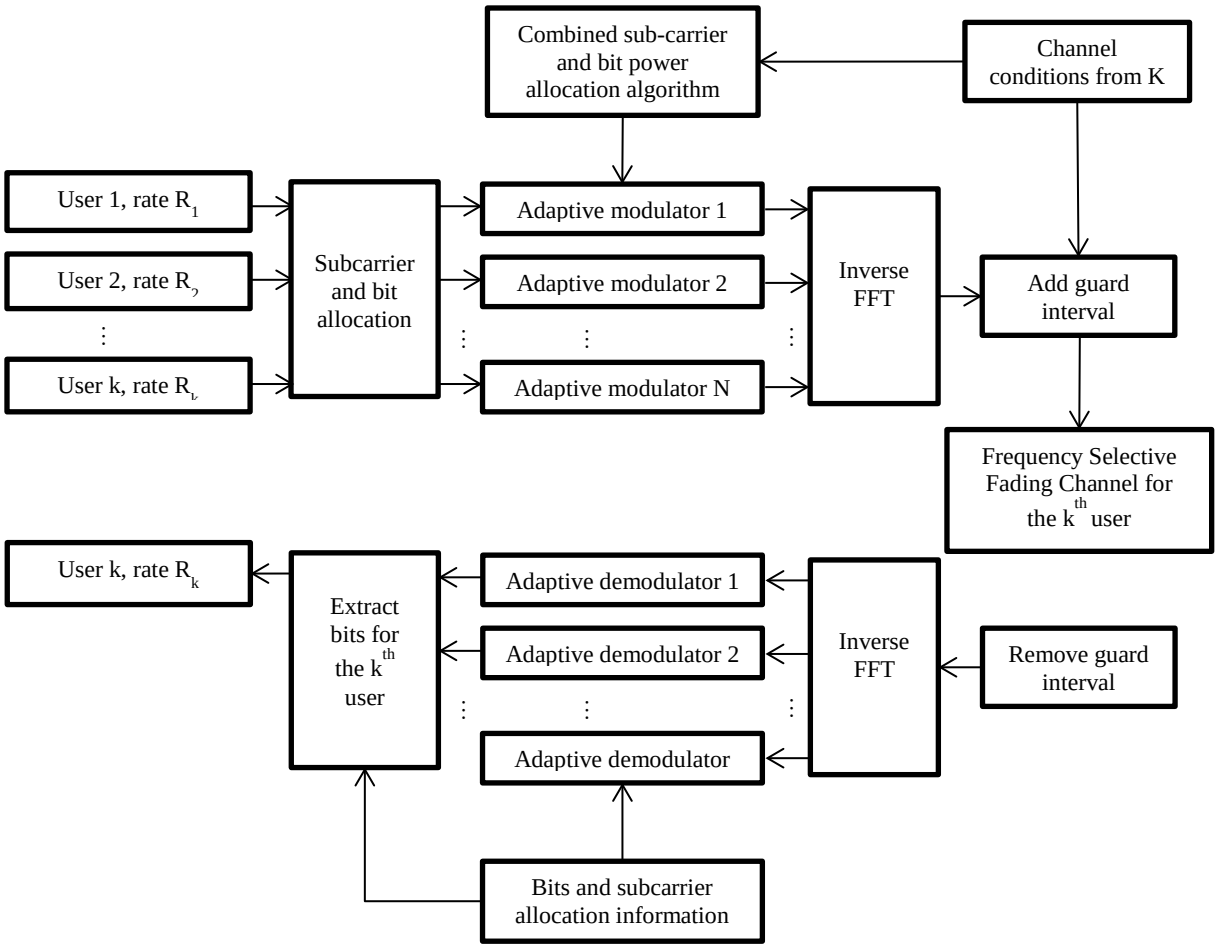

Figure 1. Block diagram of a multiuser OFDM system with subcarrier, bit, and power allocation. After [2].

2. OFDM-Based Cognitive radio

The other promising way of solving the spectrum availability crisis is to use cognitive radio (CR). CR is the wireless communication technique that allows secondary users (SU) to use the radio spectrum that is not used by primary users (PU) by sensing the radio spectrum environment. The initial main function of CR is to transmit data where a spectrum band may be available. CR does not allow a SU to use the PU's utilized spectrum but allows a SU to use the PU’s unutilized spectrum. Thus, interference control is important and is implemented using spectrum sensing and power control. Spectrum

sensing includes detecting empty spectrum that can be used by a SU. Power control is also an important technique to avoid interference. Power control includes power allocation schemes that try to maximize the capacity of CR by minimizing interference.

B. THESIS OBJECTIVE AND MOTIVATION

The main objective of this thesis is to show the Doppler effect on performance in a multiuser communication environment. Cognitive radio is an effective technology for sharing radio spectrum since secondary users try to utilize spectrum bands not being used by the primary user. The secondary user's signal can be interference to the primary user. Considering that the current wireless communication environment is very crowded and each wireless device may not be static, then frequency shifts or Doppler effects may affect both PU and SU signals. Doppler shifts can cause loss of orthogonality between the primary user and secondary user and affect both PU and SU receiver performance. In this thesis, how frequency offsets affect the performance in a two-user CR scenario is investigated.

C. LITERATURE REVIEW

Adaptive multicarrier modulation has been an active research area for quite some time. Employing repeat code and linear block code to OFDM subcarriers was discussed in [3]. Multiuser OFDM subcarrier, bit, and power allocation algorithms to minimize the total transmit power were discussed in [2]. There are also many previous studies on OFDM-based CR systems. In [4] interference detection for an OFDM-based CR system was investigated. In [5] and [6], resource allocation for an OFDM-based CR system was studied. In [7], frequency synchronization for an OFDM-based CR system was considered. In [8], [9], [10], and [11], new spectrum sensing methods based on the characteristics of the OFDM signal were proposed using either energy detection, optimal Neyman-Pearson detection, autocorrelation detection or cyclostationarity feature detection, respectively.

D. THESIS OUTLINE

This thesis is organized as follows. In Chapter II, we present background material on OFDM, QPSK (quadrature phase-shift keying), and 16QAM (16-ary quadrature amplitude modulation) modulations. In Chapter III, we discuss the notion of adaptive OFDM. We present Monte Carlo simulations that show there is no performance loss if some sub-carriers are turned off as long as the effective E_b/N_o remains the same. We also consider a few scenarios where a few bands are used in an available bandwidth. We consider the specific case where the power ratios between two signals that use the available bands are not the same while maintaining the same total power. In this chapter we also show simulations on how the primary user and secondary user can share the spectrum without causing interference with each other as long as the frequency subcarriers remain orthogonal. In Chapter IV, we introduce a classical CR scenario where a SU uses available band(s) while a PU utilizes some of the spectrum. In this chapter, we finally investigate the effect on the PU performance of Doppler shift in the SU spectrum. Finally, in Chapter V we discuss our results and offer conclusions and suggestions concerning future research.

II. GENERAL QPSK AND 16QAM MODULATION SCHEME OVER OFDM

In this chapter we discuss QPSK and 16QAM modulation schemes which are used for symbol mapping prior to OFDM signal generation. Then, we present background material on how OFDM modulation is implemented.

A. QPSK MODULATION SCHEME

QPSK is the modulation scheme using four different phase symbols as shown in Figure 2. The alphabet of QPSK symbols α_{QPSK} is given by

$$\alpha_{QPSK} = \{\pm 1 \pm j\}. \tag{2.1}$$

Each symbol represents two bits. The neighboring symbols are orthogonal to each other because of the 90-degree separation between symbols. In Figure 2, each adjacent symbol only differs by one bit. It is Gray coded to minimize bit error ratio (BER).

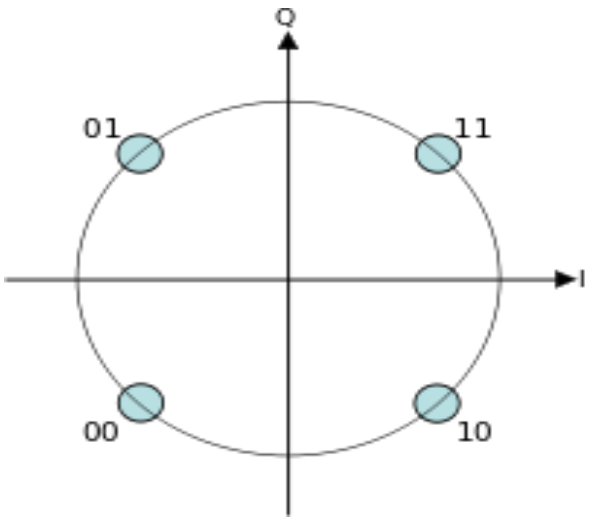

Figure 2. Constellation plot for QPSK with Gray coding.

The average symbol energy of QPSK is E_S. The probability of bit error, sometimes referred to as BER, is given by [12]

$$P_{b,QPSK} = Q\left(\sqrt{\frac{2E_b}{N_o}}\right). \tag{2.2}$$

The corresponding symbol error ratio (SER) is given by [12]

$$P_{s,QPSK} = 1-(1-P_b)^2 = 2Q\left(\sqrt{\frac{E_s}{N_o}}\right)-\left[Q\left(\sqrt{\frac{E_s}{N_o}}\right)\right]^2. \tag{2.3}$$

The second term of Equation (2.3) is negligible at high ***SNR***, so the SER equation is reduced to

$$P_{s,QPSK} \approx 2Q\left(\sqrt{\frac{E_s}{N_o}}\right). \tag{2.4}$$

B. 16QAM MODULATION SCHEME

16QAM has 16 symbols, and each symbol represents four bits. In Figure 3 the symbols shown have various phases and amplitudes. The alphabet of 16QAM symbols α_{16QAM} is given by

$$\alpha_{16QAM} = \{\pm 3 \pm 3j, \pm 3 \pm j, \pm 1 \pm 3j, \pm 1 \pm j\}. \tag{2.5}$$

In this configuration, the average energy of the 16QAM constellation E_{16QAM} is ten.

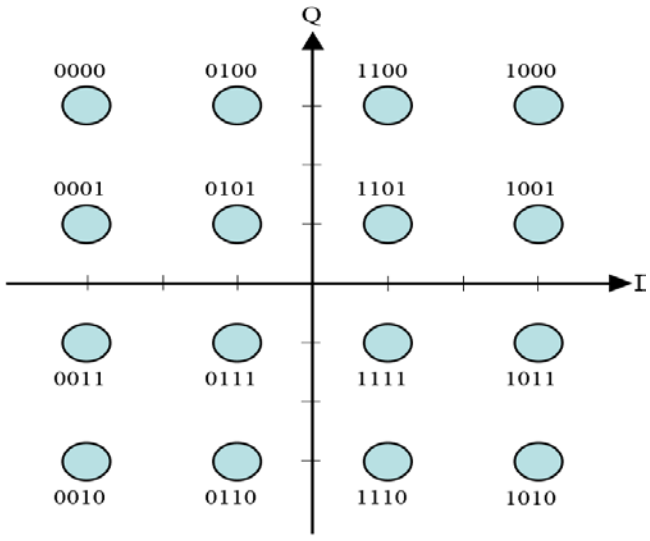

Figure 3. Constellation plot for 16-QAM with Gray coding.

The average symbol energy of 16QAM is E_S. The probability of bit error is given by [13]:

$$P_{b,16\,\mathrm{QAM}} = \frac{3}{8} Q\left(\sqrt{\frac{4E_b}{10N_o}}\right). \tag{2.6}$$

The corresponding SER is given by [13]:

$$P_{s,16\,\mathrm{QAM}} = \frac{3}{2} Q\left(\sqrt{\frac{E_s}{10N_o}}\right). \tag{2.7}$$

C. OFDM SCHEME

In this section, we first discuss OFDM transmission and reception. OFDM uses subcarriers with frequency separation $1/T$, where T is the symbol period. The information α_κ to be sent on each subcarrier k is multiplied by the corresponding carrier as given by

$$g_K(t) = \frac{1}{\sqrt{T}} e^{\frac{j2\pi kt}{T}} \omega(t) \tag{2.8}$$

where $\omega(t)$ is a rectangular window over [0 T]. Mathematically, the transmit signal $s(t)$ is given by

$$\begin{aligned} s(t) &= \alpha_0 g_0(t) + \alpha_1 g_1(t) + \cdots + \alpha_{K-1} g_{K-1}(t) \\ &= \sum_0^{K-1} \alpha_K g_K(t) \\ &= \frac{1}{\sqrt{T}} \sum_0^{K-1} \alpha_K e^{\frac{j2\pi kt}{T}} \omega(t). \end{aligned} \tag{2.9}$$

Each information signal α_κ multiplies the complex sinusoid having the frequency k/T. The modulated subcarriers are added, and the resultant signal is sent out as $s(t)$. In an OFDM receiver, the received signal is multiplied by a bank of correlators and is integrated over the symbol period. The concept of an OFDM modulator is shown in Figure 4. Binary data are mapped by subcarrier symbols using a modulation scheme such as QPSK and 16QAM. The resulting mapping is fed into the inverse fast Fourier transform (FFT) from baseband carrier modulation. The guard interval is added and pulse shaping is performed by the digital/analog (D/A) converter circuitry. Eventually, the analog signals are multiplied by the carrier signals, and the resulting I and Q channels are added.

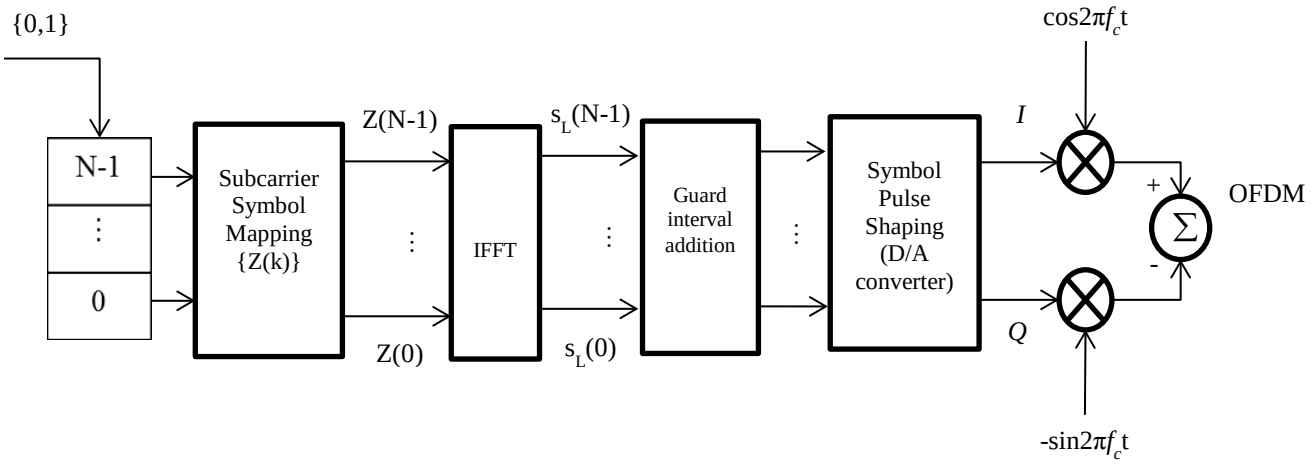

Figure 4. Block diagram of an OFDM modulator [14].

III. ADAPTIVE OFDM SIMULATIONS

Usually OFDM uses the same subcarrier modulation scheme for each channel. In adaptive OFDM modulation, any subcarrier may be turned off for the radio to truly implement adaptive modulation. Adaptive OFDM may be used in cognitive radio where the secondary users are allowed to use unused frequency bands allocated to the primary users. Thus, for OFDM to work for a SU, there is a need to turn off subcarriers in frequency bands that are used by a PU. In this chapter, we illustrate a few cases where we turn off some subcarriers while keeping the effective E_b/N_o the same. By Monte Carlo simulation, we show that there is no performance degradation if power reallocation is performed. In order to turn off certain subcarriers, we intentionally set the amplitude of those carriers to zero prior to the inverse FFT. The inverse FFT generates the OFDM signal where it is apparent that some carriers are turned off. The fact that some carriers are turned off is not apparent in the time domain. However, we present simulated spectra in the frequency domain where some carriers are clearly used and others are turned off. With the use of Monte Carlo simulations using Matlab, we are able to show BER/SER performance for scenarios where subcarriers are turned off and compare them to theoretical BER/SER expressions as a function of increasing ***SNR***.

A. EIGHT SUBCARRIERS (4 ON, 4 OFF)

1. QPSK Modulation with OFDM

In this scenario, we use QPSK modulation with OFDM, where the first four subcarriers are used and the next four subcarriers are turned off. In Table 1 the utilization of the subcarriers is shown. Clearly, QPSK symbols are sequentially mapped to the utilized subcarriers. A Monte Carlo simulation using 4×10^5 QPSK symbols is performed to produce two power spectral densities (PSDs) of the symbol sequence. Since the four subcarriers are turned off, the inverse FFT are padded by the same amount of zero-symbols. In other words, the eight-point inverse FFT operates on four QPSK symbols and four zeros. The unfiltered PSD is shown in Figure 5(a), and a Welch-estimated [15] version is shown in Figure 5(b).

Table 1. Subcarrier utilization of eight subcarrier OFDM: four are used for QPSK and four are turned off.

SC 1	SC 2	SC 3	SC 4	SC 5	SC 6	SC 7	SC 8
QPSK Symbol	QPSK Symbol	QPSK Symbol	QPSK Symbol	OFF	OFF	OFF	OFF

It is clear in Figure 5 that the first four subcarriers are utilized in the frequency spectrum, and the other four subcarriers are turned off. The spectral content spilling into the supposedly unutilized bands is actually sidelobes from the four utilized bands. Since these subcarriers are orthogonal, the spectral spillage does not produce errors (provided orthogonality is preserved). The BER and SER for this scenario (4-ON and 4-OFF subcarriers with QPSK-OFDM) are shown in Figure 6. We observe that the BER/SER result from Monte Carlo simulation is in good agreement with the theoretical BER/SER for QPSK modulation as dictated by Equation (2.2) and Equation (2.4).

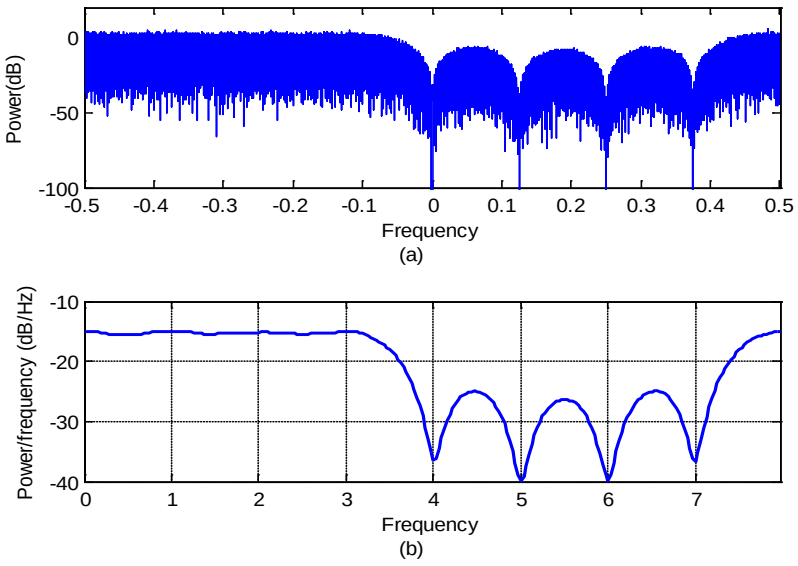

Figure 5. PSDs for randomly generate QPSK-OFDM symbols for the eight-subcarrier (4-ON, 4-OFF) scenario: (a) Unfiltered; (b) Welch estimated PSD.

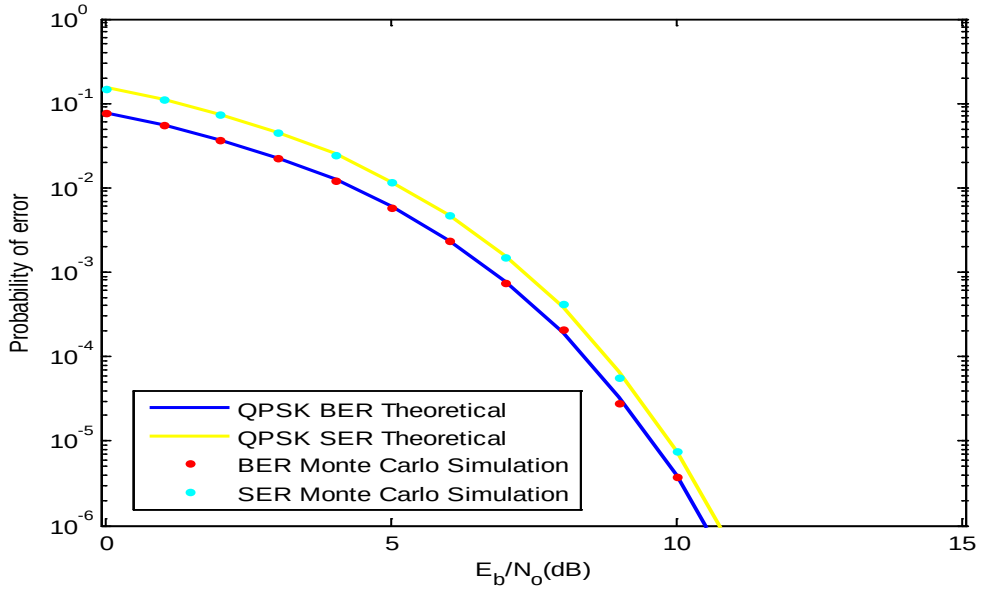

Figure 6. Performance curves for the eight subcarrier (4 ON, 4 OFF, QPSK-OFDM) scenario vs. E_b/N_o.

2. 16QAM Modulation with OFDM

In this scenario, we use 16QAM modulation with OFDM, where the first four subcarriers are used and the next four subcarriers are turned off. In Table 2 the utilization of the subcarriers is shown. Clearly, the symbols are sequentially mapped into the utilized subcarriers. A Monte Carlo simulation using 4×10^5 symbols is performed to produce two PSDs of the symbol sequence. Since the four subcarriers are turned off, the inverse FFT is padded by the same amount of zero-symbols. In other words, the eight-point inverse FFT operates on four 16QAM symbols and four zeros. The unfiltered PSD is shown in Figure 7(a), and a Welch-estimated version is shown in Figure 7(b).

Table 2. Subcarrier utilization of eight subcarrier OFDM: four are used for 16QAM and four are turned off.

SC 1	SC 2	SC 3	SC 4	SC 5	SC 6	SC 7	SC 8
16QAM Symbol	16QAM Symbol	16QAM Symbol	16QAM Symbol	OFF	OFF	OFF	OFF

It is clear in Figure 7 that the first four subcarriers are utilized in the frequency spectrum, and the other four subcarriers are turned off. The spectral content spilling into the supposedly unutilized bands is actually sidelobes from the four utilized bands. Since these subcarriers are orthogonal, the spectral spillage does not produce errors (provided orthogonality is preserved). The BER and SER for this scenario (4-ON and 4-OFF subcarriers with 16QAM-OFDM) are shown in Figure 8. We observe that the BER/SER resulting from Monte Carlo simulation is in good agreement with the theoretical bit error rate for 16QAM modulation as dictated by Equation (2.6) and (2.7).

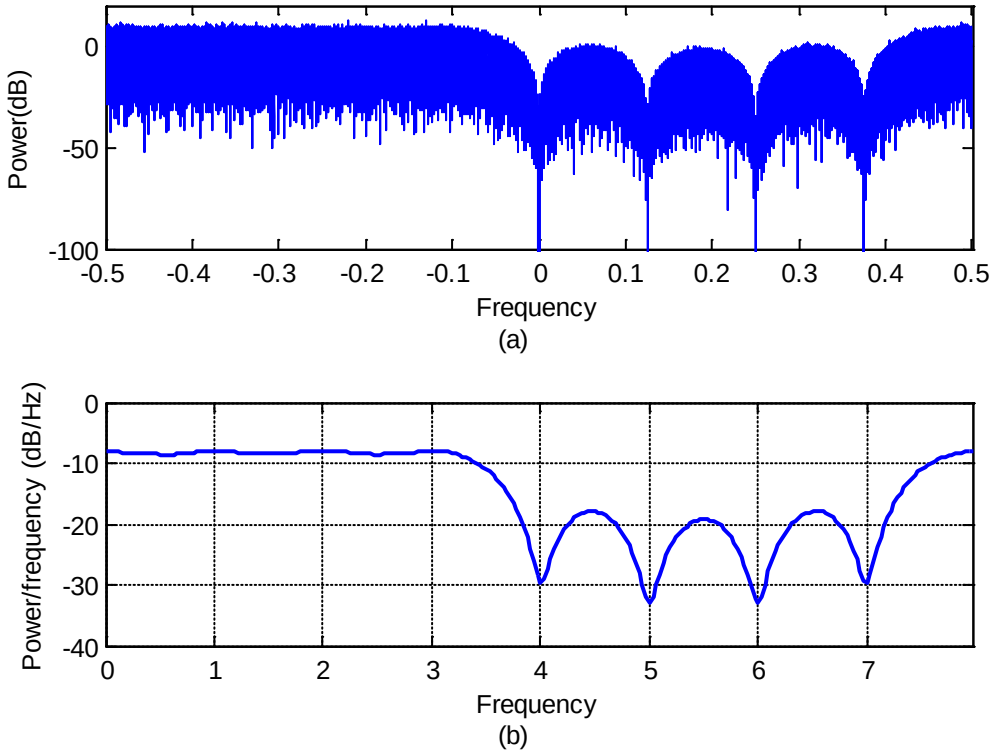

Figure 7. PSDs for randomly generated 16QAM-OFDM symbols for the eight-subcarrier (4-ON, 4-OFF) scenario: (a) Unfiltered; (b) Welch estimated PSD.

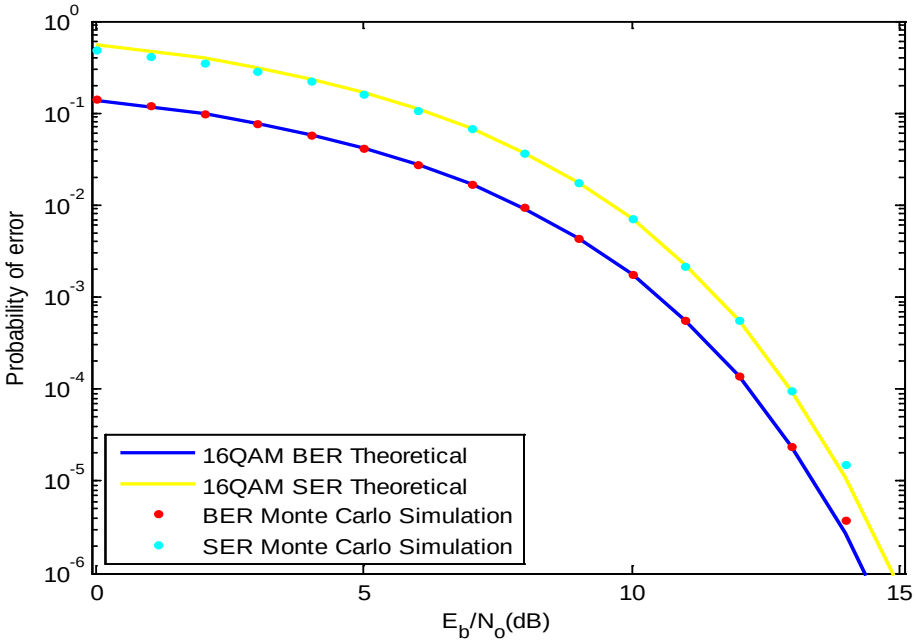

Figure 8. Performance curves for the eight subcarrier (4 ON, 4 OFF, 16QAM-OFDM) scenario vs. E_b/N_o.

B. TWELVE SUBCARRIER SCENARIO (4 ON, 4 OFF, 4 ON)

In this scenario, we set a 12-subcarrier OFDM spectral allocation. We allow for the first four subcarriers and last four subcarriers to be used. The middle four subcarriers are turned off. In other words, the set of channels in the middle is turned off.

1. QPSK Modulation with OFDM

We show in Table 3 the utilization of the OFDM channels in which eight subcarriers are used and four are turned off.

Table 3. Subcarrier utilization of 12 subcarrier OFDM: first four and last four subcarriers are used for QPSK and the middle four subcarriers are turned off.

SC 1~4	SC 5~8	SC 9~12
QPSK Symbols	OFF	QPSK Symbols

In Figure 9 it is clear that the nulls of the spectra correspond to the four subcarriers in the middle bands. Since these subcarriers are orthogonal, the spectral spillage does not produce errors if these bands spilling into the supposedly unutilized bands are utilized (provided orthogonality is preserved). The BER and SER for this scenario (4-ON, 4-OFF, and 4-ON subcarriers with QPSK-OFDM) are shown in Figure 10. We observe that the BER/SER resulting from Monte Carlo simulation is in good agreement with the theoretical BER/SER for QPSK modulation as dictated by Equation (2.2) and (2.4).

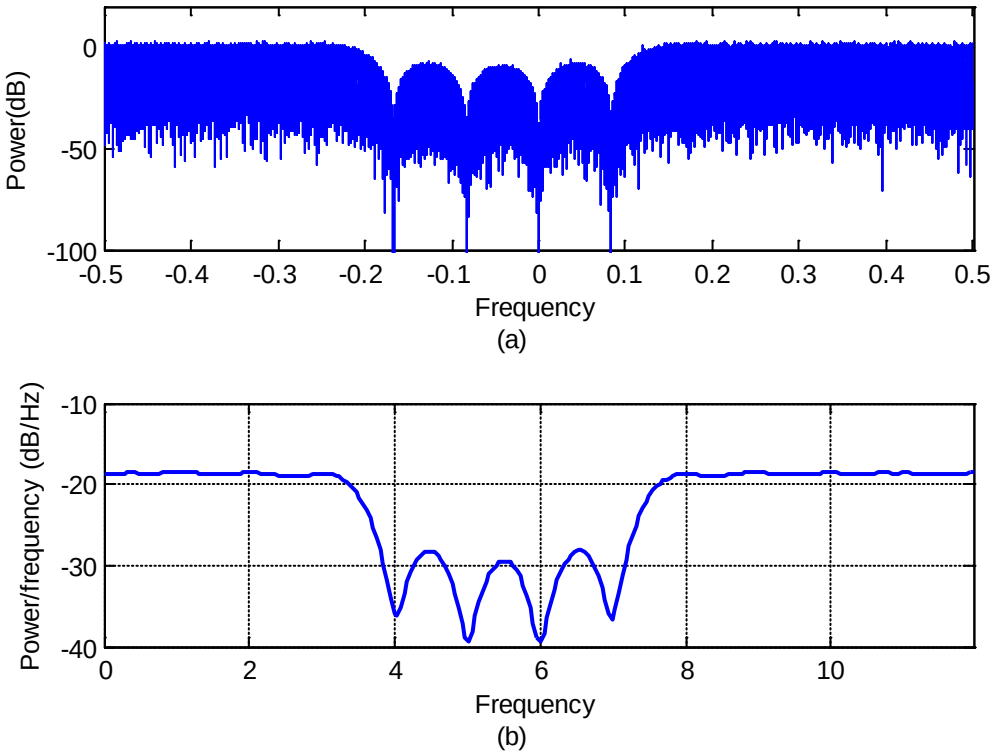

Figure 9. PSDs for randomly generated QPSK-OFDM symbols for the 12-subcarrier (4-ON, 4-OFF, 4-ON) scenario: (a) Unfiltered; (b) Welch estimated PSD.

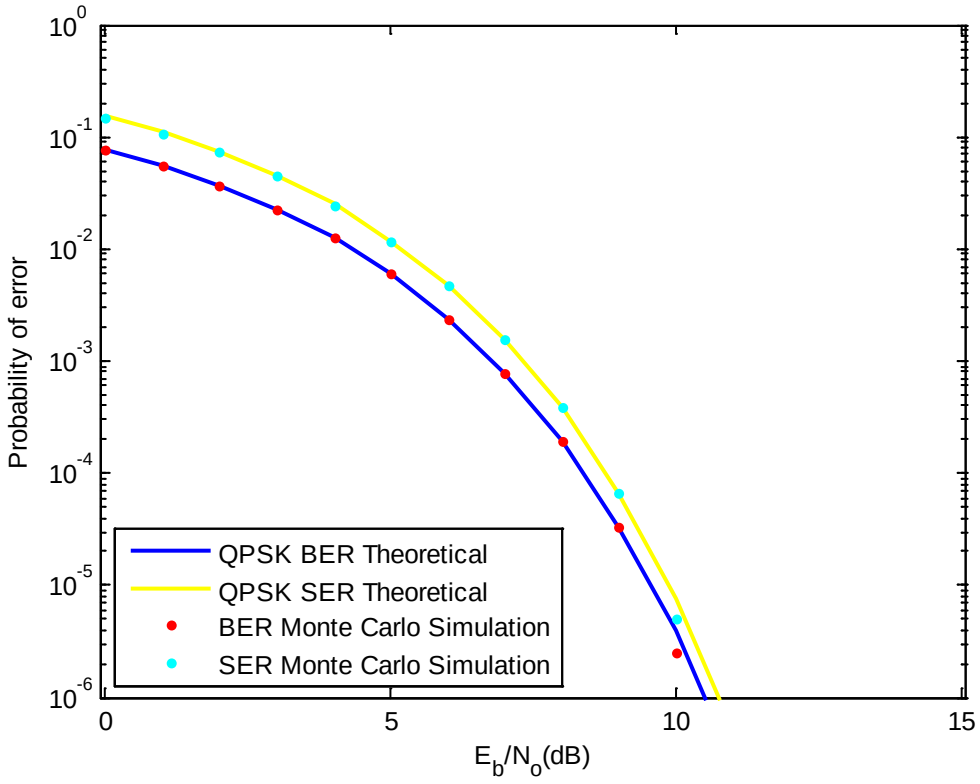

Figure 10. Performance curves for the 12 subcarrier (4 ON, 4 OFF, 4 ON, QPSK-OFDM) scenario vs. E_b/N_o.

2. 16QAM Modulation with OFDM

We show in Table 4 the utilization of the OFDM channels in which eight subcarriers are used and four are turned off.

Table 4. Subcarrier utilization of 12 subcarrier OFDM: first four and last four subcarriers are used for 16QAM and the middle four subcarriers are turned off.

SC 1~4	SC 5~8	SC 9~12
16QAM Symbols	OFF	16QAM Symbols

In Figure 11 it is clear that the nulls of the spectra correspond to the four subcarriers in the middle bands. Since these subcarriers are orthogonal, the spectral spillage does not produce errors (provided orthogonality is preserved). The BER and SER for this scenario (4-ON, 4-OFF and 4-ON subcarriers with 16QAM-OFDM) are shown in Figure 12. We observe that BER/SER resulting from Monte Carlo simulation is in good agreement with the theoretical BER/SER for 16QAM modulation as dictated by Equation (2.6) and (2.7).

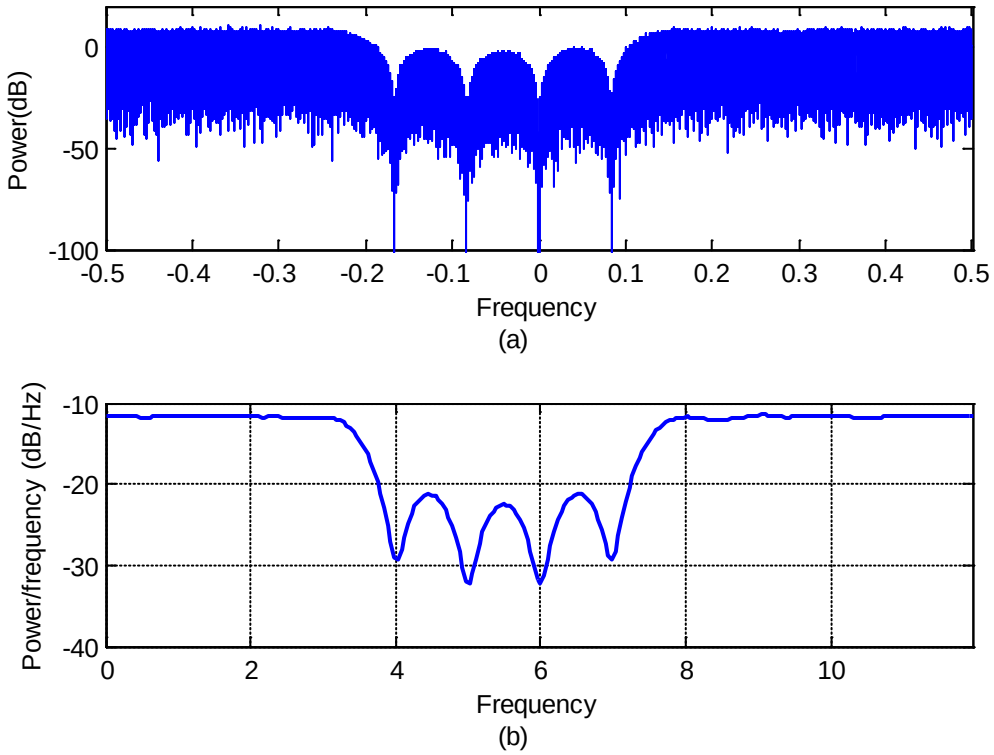

Figure 11. PSDs for randomly generated 16QAM-OFDM symbols for the 12-subcarrier (4-ON, 4-OFF, 4-ON) scenario: (a) Unfiltered; (b) Welch estimated PSD.

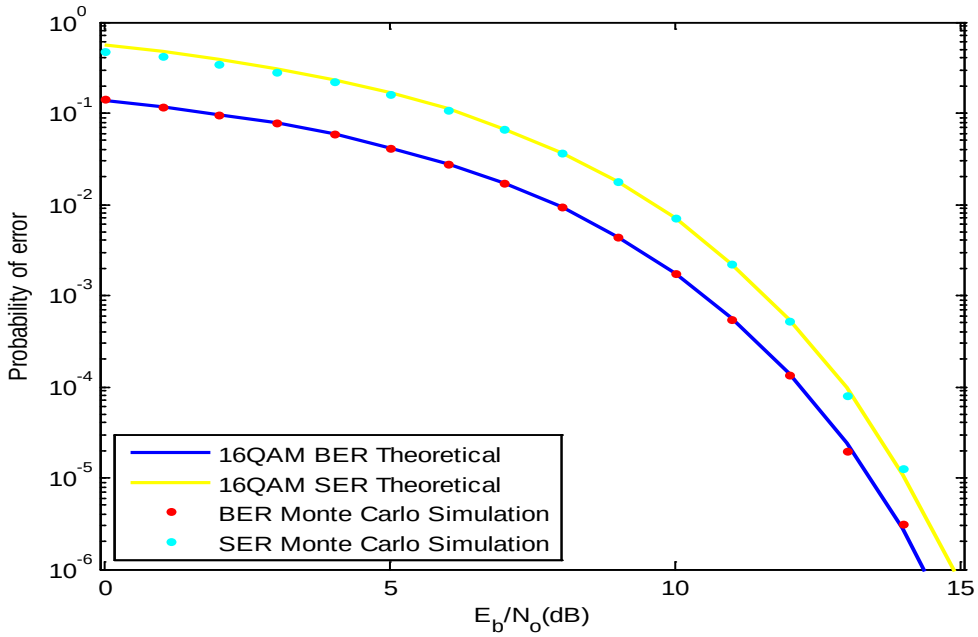

Figure 12. Performance curves for the 12 subcarrier (4 ON, 4 OFF, 4 ON, 16QAM-OFDM) scenario vs. E_b/N_o.

C. SIXTEEN SUBCARRIER SCENARIO (4 ON, 4 OFF, 4 ON, 4 OFF)

In this scenario, we set a 16-subcarrier OFDM spectrum. We allow for the first four subcarriers and third four subcarriers to be used. The second four subcarriers and last four subcarriers are turned off.

1. QPSK Modulation with OFDM

We show in Table 5 the utilization of the OFDM channels in which eight subcarriers are used and eight are turned off.

Table 5. Subcarrier utilization of 16 subcarrier OFDM: first four and third four subcarriers are used for QPSK and the second four and last four subcarriers are turned off.

SC 1~4	SC 5~8	SC 9~12	SC 13~16
QPSK Symbols	OFF	QPSK Symbols	OFF

We observe that low power sidelobes spill into two white spaces in Figure 13. Since these subcarriers are orthogonal, the spectral spillage does not produce errors (provided orthogonality is preserved). The BER and SER for this scenario (4-ON, 4-OFF, 4-ON and 4-OFF subcarriers with QPSK-OFDM) are shown in Figure 14. We observe that the BER/SER resulting from Monte Carlo simulation is in good agreement with the theoretical BER/SER for QPSK modulation as dictated by Equation (2.2) and (2.4).

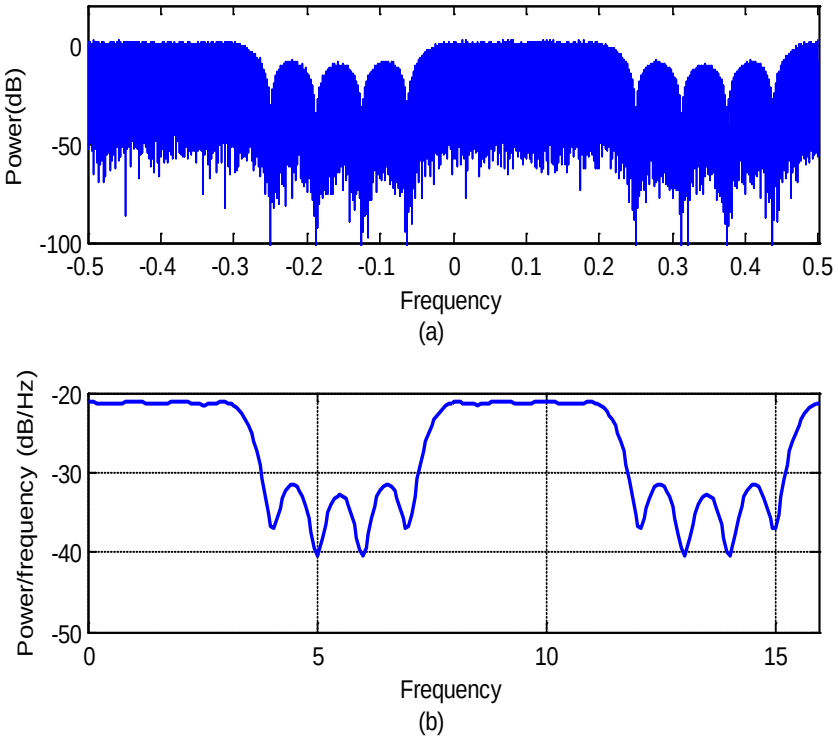

Figure 13. PSDs for randomly generated QPSK-OFDM symbols for the 16-subcarrier (4-ON, 4-OFF, 4-ON, 4-OFF) scenario: (a) Unfiltered; (b) Welch estimated PSD.

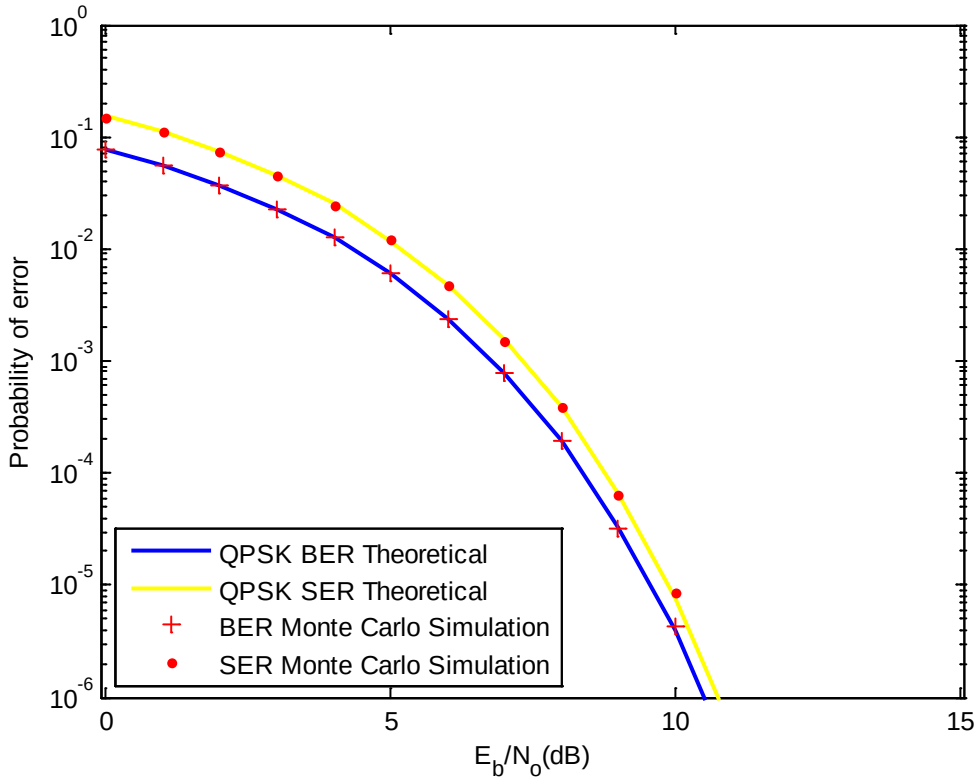

Figure 14. Performance curves for the 16 subcarrier (4 ON, 4 OFF, 4 ON, 4 OFF, QPSK-OFDM) scenario vs. E_b/N_o.

2. 16QAM Modulation with OFDM

We show in Table 6 the utilization of the OFDM channels in which eight subcarriers are used and eight are turned off.

Table 6. Subcarrier utilization of 16 subcarrier OFDM: first four and third four subcarriers are used for 16QAM and the second four and last four subcarriers are turned off.

SC 1~4	SC 5~8	SC 9~12	SC 13~16
16QAM Symbols	OFF	16QAM Symbols	OFF

We observe that low power sidelobes spill into two white spaces in Figure 15. Since these subcarriers are orthogonal, the spectral spillage does not produce errors (provided orthogonality is preserved). The BER and SER for this scenario (4-ON, 4-OFF, 4-ON and 4-OFF subcarriers with 16QAM-OFDM) are shown in Figure 16. We observe that the BER/SER resulting from Monte Carlo simulation is in good agreement with the theoretical BER/SER for 16QAM modulation as dictated by Equation (2.6) and (2.7).

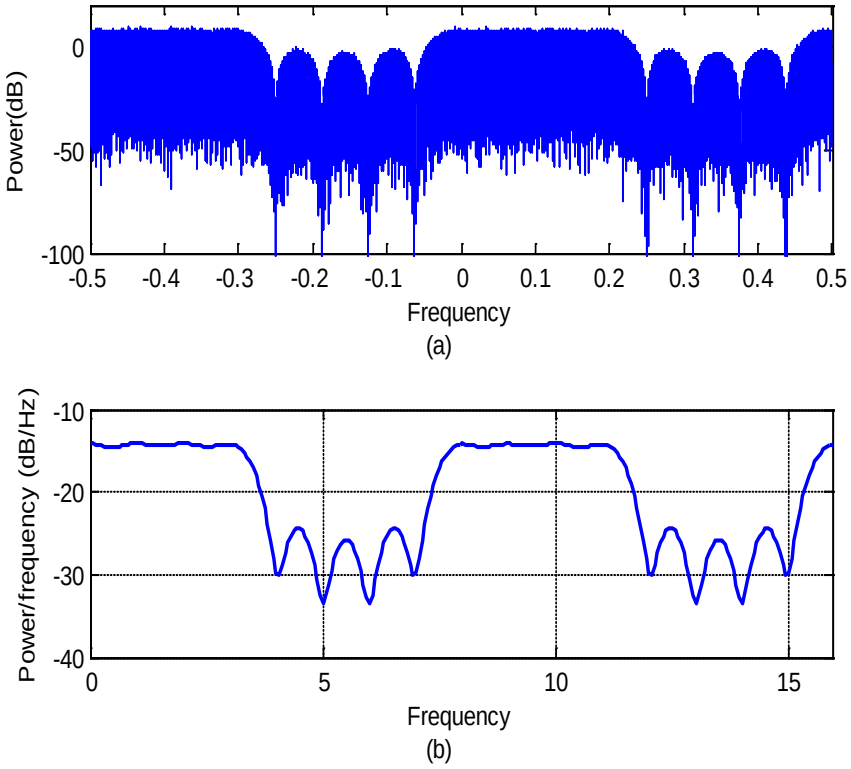

Figure 15. PSDs for randomly generate 16QAM-OFDM symbols for the 16-subcarrier (4-ON, 4-OFF, 4-ON, 4-OFF) scenario: (a) Unfiltered; (b) Welch estimated PSD.

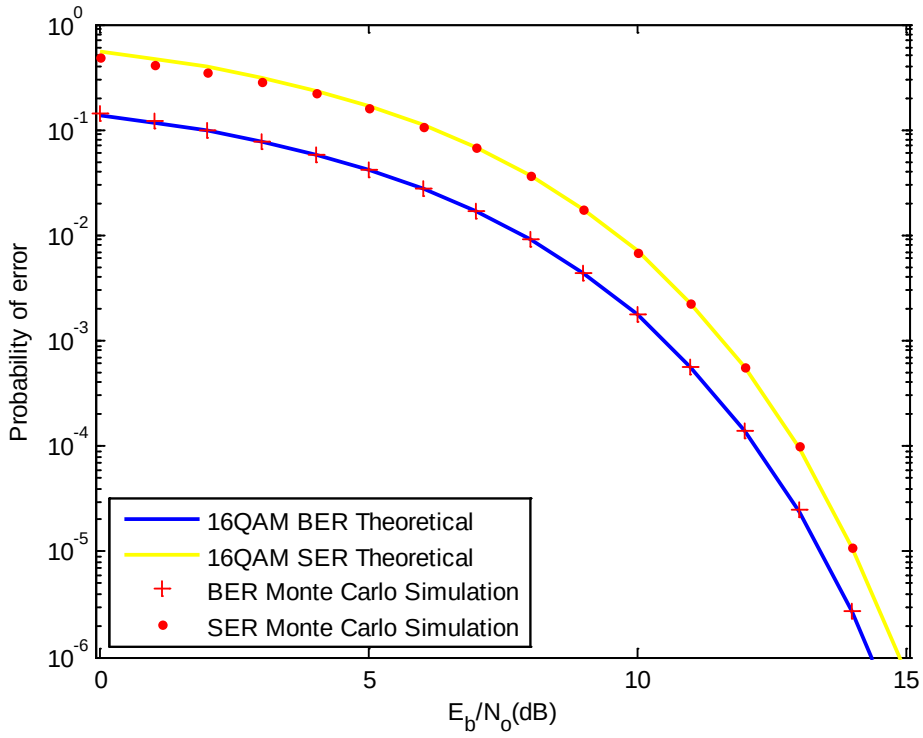

Figure 16. Performance curves for the 16 subcarrier (4 ON, 4 OFF, 4 ON, 4 OFF, 16QAM-OFDM) scenario vs. E_b/N_o.

D. CHANGING POWER RATIO ON 12 SUBCARRIER SCENARIO (4 ON, 4 OFF, 4 ON)

In this scenario, we set a 12-subcarrier OFDM spectral allocation. We allow for the first four subcarriers and last four subcarriers to be used; but in this scenario, we adjusted the average power ratio between the first four subcarriers and last four subcarriers while the sum of total subcarrier power remained constant. Recall the middle four subcarriers are turned off. In other words, the set of channels in the middle is not used and the two bands that are used have different power.

1. QPSK Modulation with OFDM

We show in Table 3 the utilization of the OFDM channels in which eight subcarriers are used and four are turned off. First and last four subcarriers are set to different average power levels. We increase the power of the first four subcarriers and

decrease the power of the last four subcarriers to make an *N* to 1 power ratio between the two sets of subcarriers.

We observe that the BER/SER pair gets worse as the power ratio is increased when we fix E_b/N_o = 5 dB in Figure 17.

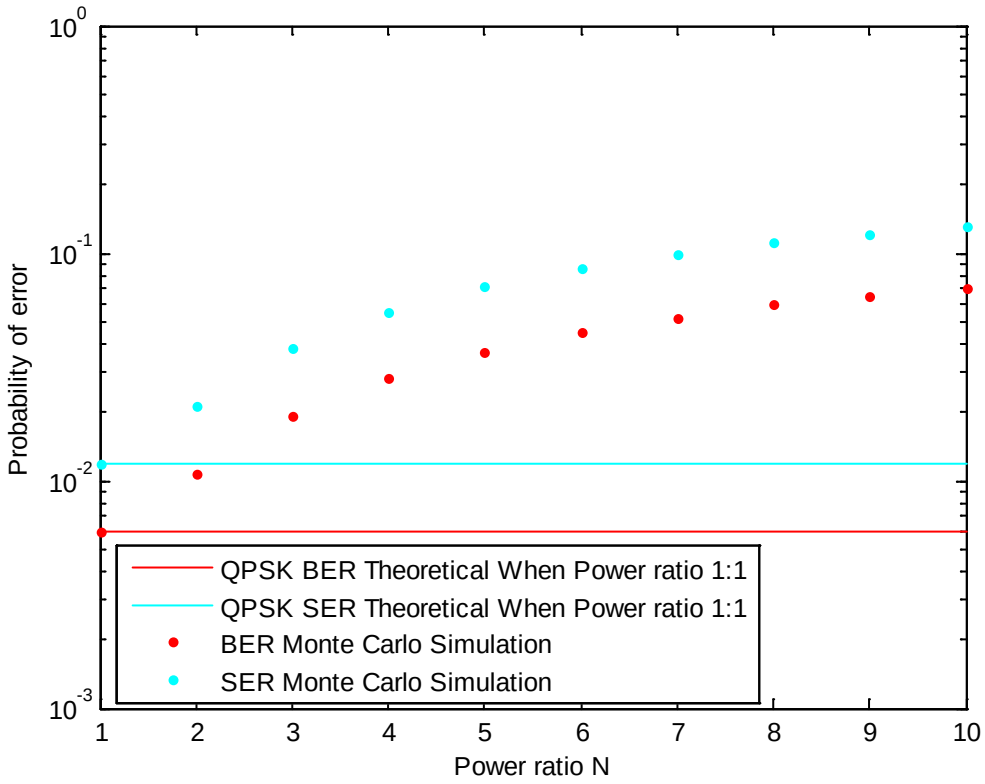

Figure 17. Performance curves for the 12 subcarrier (4 ON, 4 OFF, 4 ON, QPSK-OFDM) scenario vs. power ratio N at E_b/N_o = 5 dB.

In Figure 18, we observe that the BER/SER resulting from Monte Carlo simulation is in good agreement with the theoretical bit/symbol error rate for QPSK modulation as dictated by Equation (2.2) and (2.4) only when the power ratio is 1:1. As we increase *N*, BER/SER results worsen.

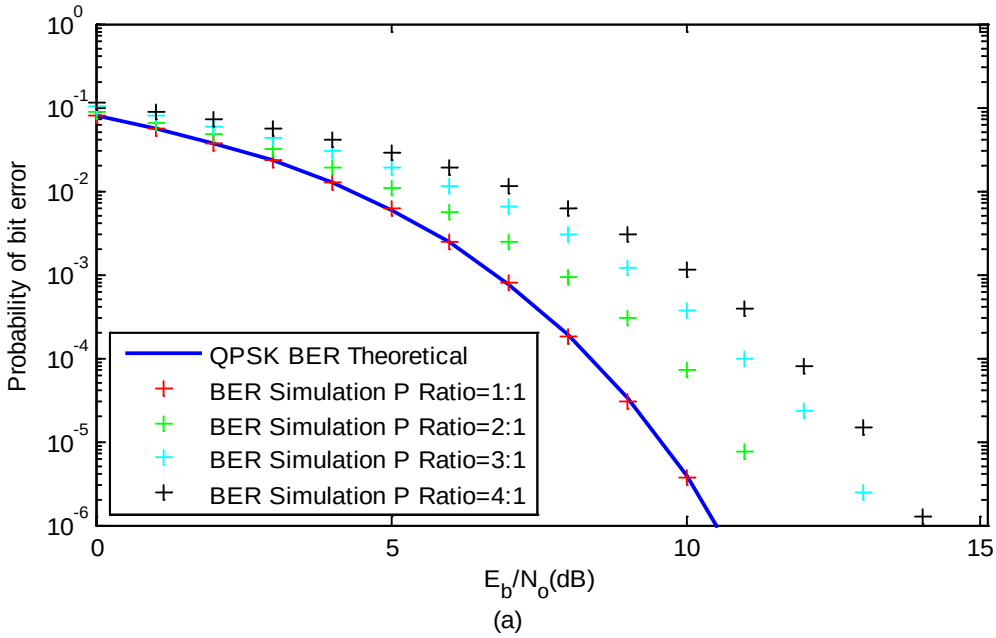

(a)

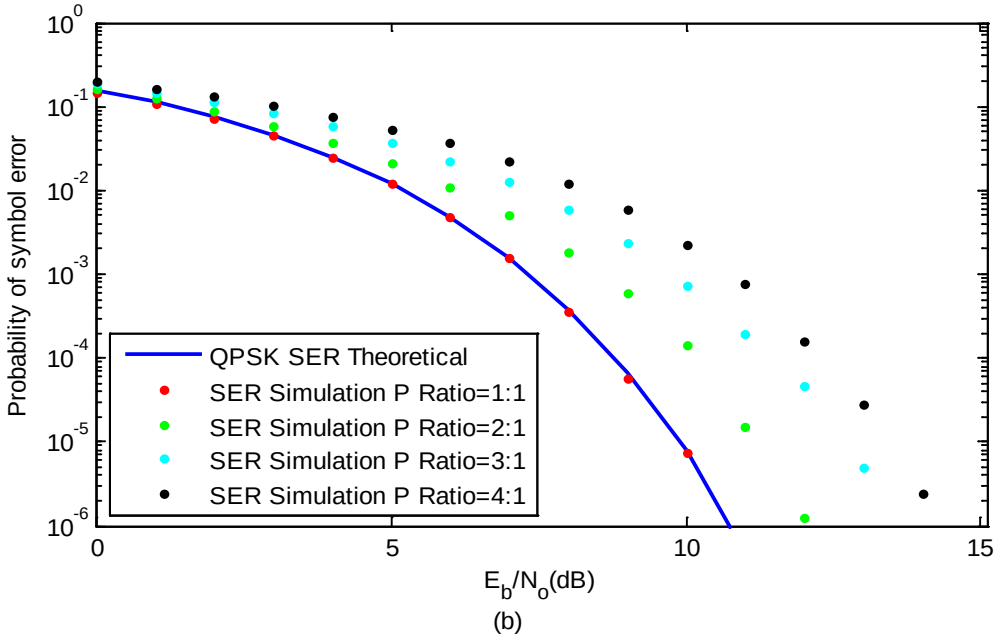

(b)

Figure 18. Performance curves for the 12 subcarrier (4 ON, 4 OFF, 4 ON, QPSK-OFDM) scenario vs. E_b/N_o. as a function of power ratio: (a) BER; (b) SER.

The point of the simulation results in this section is to show that equal power allocation is best for OFDM using the same modulation and an equal number of subcarriers (when two or more bands are available to use).

2. 16QAM Modulation with OFDM

We show in Table 4 the utilization of the OFDM channels in which eight subcarriers are used and four are turned off. The first and last four subcarriers are set to different average power levels. We increase the power of the first four subcarriers and decrease the power of the last four subcarriers to make an *N*-to-1 power ratio between the two sets of subcarriers.

We observe the BER/SER pair gets worse as the power ratio is increased when we fix E_b/N_o = 5 dB in Figure 19.

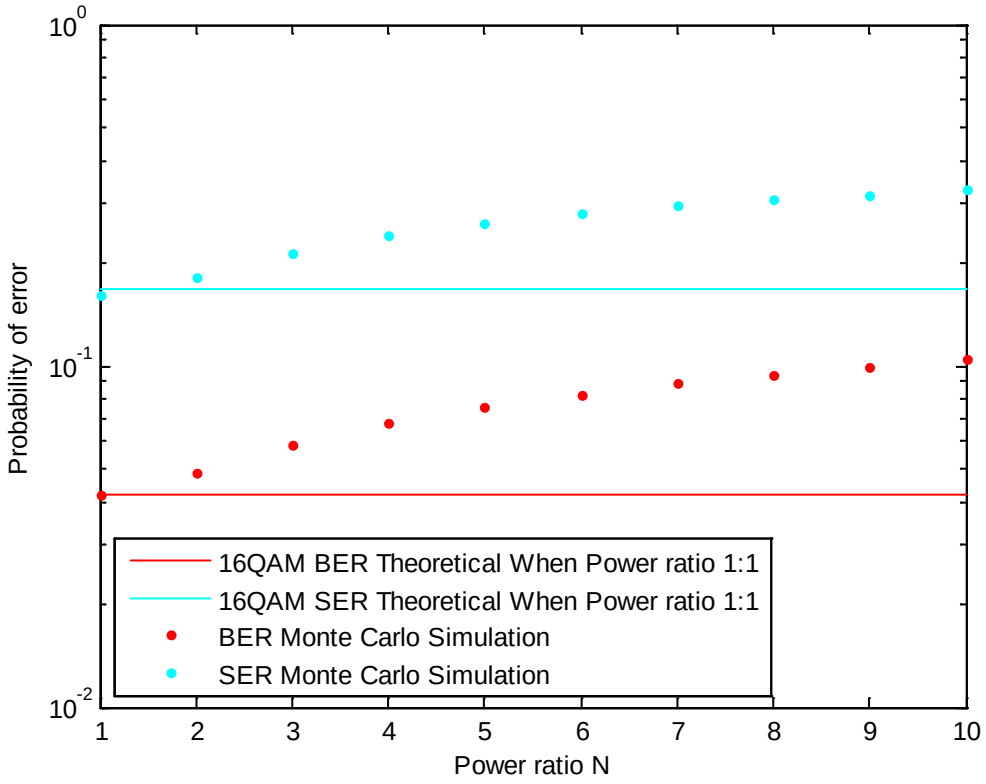

Figure 19. Performance curves for the 12 subcarrier (4 ON, 4 OFF, 4 ON, 16QAM-OFDM) scenario vs. power ratio N at E_b/N_o = 5 dB.

In Figure 20, we observe that BER/SER resulting from Monte Carlo simulation is in good agreement with the theoretical bit/symbol error rate for 16QAM modulation as dictated by Equation (2.6) and (2.7) only when the power ratio is 1:1. As we increase *N*, the BER/SER results worsen.

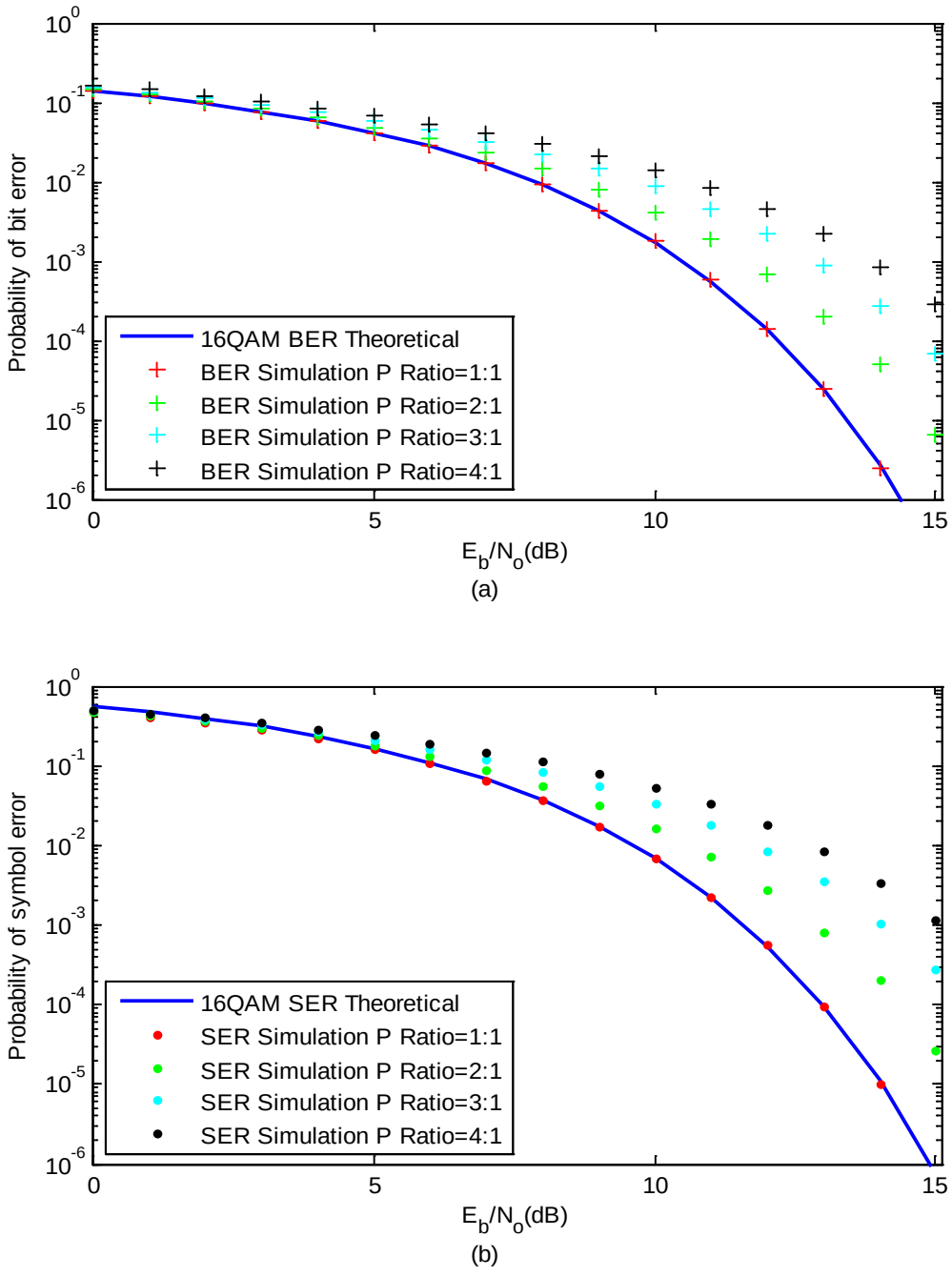

Figure 20. Performance curves for the 12 subcarrier (4 ON, 4 OFF, 4 ON, 16QAM-OFDM) scenario vs. E_b/N_o. as a function of power ratio: (a) BER; (b) SER.

THIS PAGE INTENTIONALLY LEFT BLANK.

IV. TWO-USER SCENARIO (CR SCENARIO)

In this chapter we investigate what happens when a primary user using some of its available bandwidth is joined by a secondary user which decides to use some of the available bandwidth not being used by the PU. This is the classic two-user cognitive radio scenario. The un-utilized band which corresponds to unused subcarriers is called a spectral hole or white space. Although multiple users may be actually interested in using the spectrum, extraction of performance curves for a multi-user scenario via Monte Carlo simulations becomes very resource intensive and is beyond the scope of this work. As such, we concentrate on a classic two-user scenario where one is a PU and the other is a SU.

In reality, the PU may actually have a different modulation from the SU. Clearly, we cannot explore all combinations of modulations between PU and SU. In fact, in some CR literature, it is recommended for efficient utilization of the spectrum that both users use the same type of modulation. Indeed, most CR suggests adaptive OFDM, i.e., OFDM where one or a group of subcarriers may be turned off. In this work, we assume that both the PU and SU use the same OFDM type of modulation. We then investigate the effect of Doppler shift of the SU modulation to the PU's performance. The concept diagram of transmission and reception in a two-user CR is shown in Figure 21.

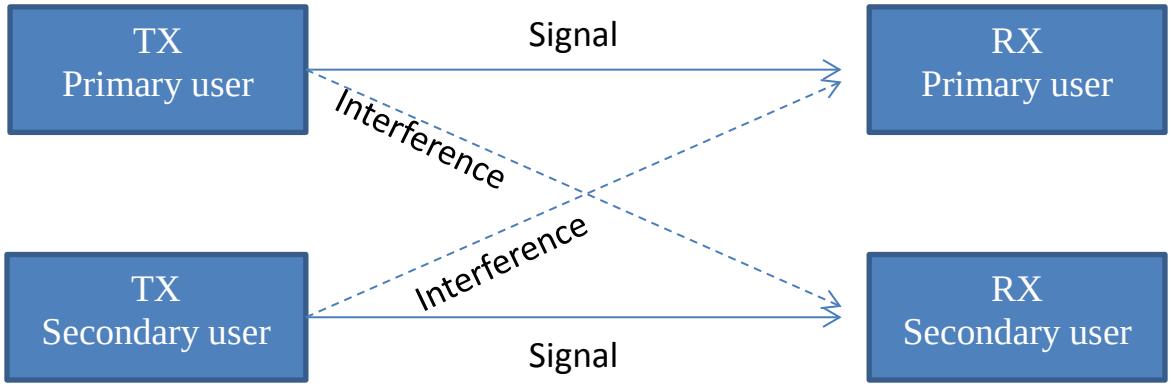

Figure 21. Concept diagram of transmission and reception in a two-user CR where Doppler shifts may result in interferences.

OFDM signals that are offset in frequency due to Doppler shift may be sensitive to carrier frequency offset. In a typical wireless communication system, the signal to be transmitted is upconverted to a carrier frequency prior to transmission. The receiver is expected to tune to the same carrier frequency for downconverting the signal to baseband, prior to demodulation. However, due to Doppler shift, the received carrier frequency may not be same as the downconverter carrier frequency of the receiver. When this happens, the received baseband signal is offset (from baseband center frequency which is usually DC) by f_δ. If the transmitted signal $s(t)$ is Doppler-shifted by frequency offset f_δ, the received signal $y(t)$ is given by

$$y(t) = s(t)e^{j2\pi f_\delta t}. \tag{4.1}$$

1. Without Frequency Offset or Doppler shift

It is possible for the SU and PU to interfere with one another. When the PU and SU received signals have no Doppler shift, then SU/PU BER and SER performances should clearly be in good agreement with expected theoretical results provided they implement the same OFDM modulation type (as was discussed earlier). In fact this is true regardless of their power ratio. This is because the subcarriers remain orthogonal. We perform various simulations where a PU uses a channel (four-subcarrier portion) of the spectrum and a SU uses two channels (two four subcarrier channels). In the next section, we discuss some of these results along with the results where the Doppler shift is present.

2. With Frequency Offset or Doppler shift

In this section, we evaluate the impact of frequency offset or Doppler shift due to relative motion between transmitter and receiver. The Doppler shift results in what could be thought of as Inter Carrier Interference (ICI) while receiving OFDM modulated symbols. To investigate the relation between ***SIR*** and performance in terms of BER/SER as a function of frequency offset, we perform simulations under various ***SIR*** (-6 dB, -3 dB, 0 dB, 3 dB, 6 dB, 10 dB). More specifically, we vary the frequency offset of the SU over PU's available bandwidth by 0.1%, 0.5%, 1%, 2% and 5%. For example, if the entire bandwidth is 100 MHz, then 1% Doppler shift is 1MHz. However, in our

simulations, for the purposes of convenience, the entire available bandwidth is normalized to one.

We consider the case when ***SIR*** = -6 dB, which means the sum of the SU signal power is about four times larger than the sum of the PU signal power while we vary the Doppler offset. This scenario is depicted in Figure 22. In Figure 23, we show the spectra when the SU Doppler offset is 1% of the PU's available bandwidth. Notice the slight frequency shift (as compared to the SU spectrum from Figure 22). This means that the subcarriers of the PU and SU added signal are not orthogonal. Since these subcarriers are not orthogonal, the spectral spillage produces errors. The BER and SER for various frequency offsets are shown in Figure 24. We observe that the BER/SER pair resulting from Monte Carlo simulation is not in good agreement with the theoretical BER/SER for QPSK modulation as dictated by Equation (2.2) and (2.4) except without the frequency offset. The BER and SER get worse as the frequency offset gets worse.

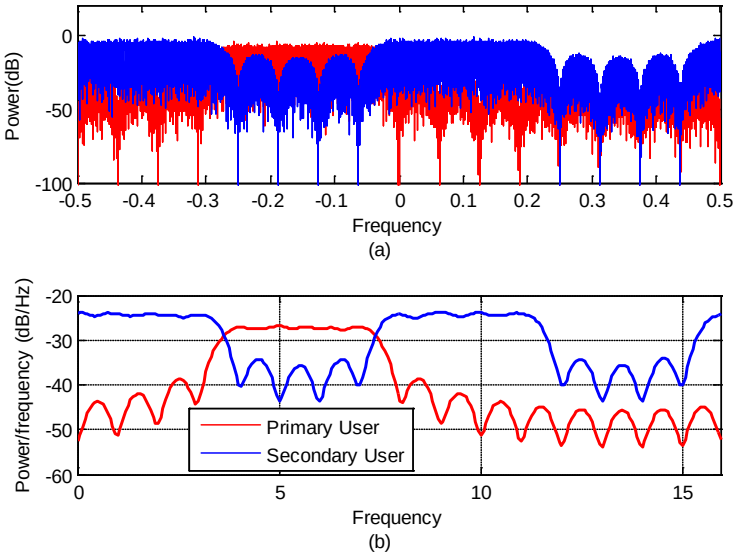

Figure 22. PSDs of PU and SU employing QPSK-OFDM where the PU to SU power ratio is -6 dB (***SIR***): (a) Unfiltered PSD; (b) Welch estimated PSD.

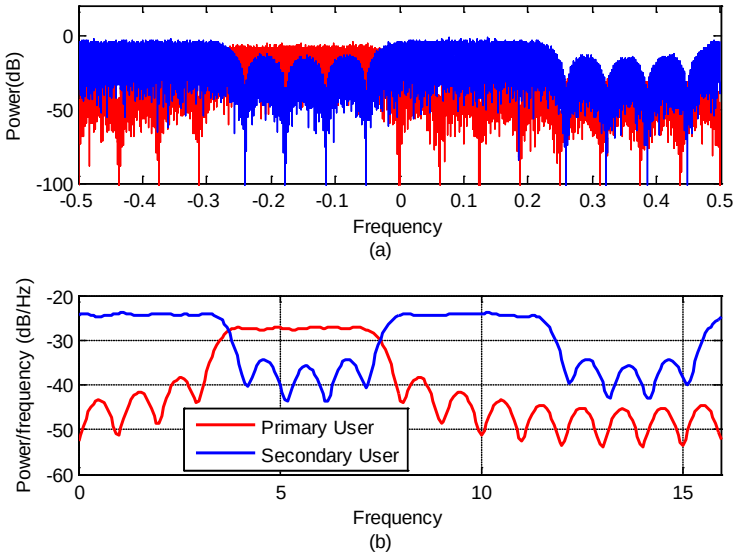

Figure 23. PSDs of PU and SU employing QPSK-OFDM where the PU to SU power ratio is -6 dB (***SIR***) and SU is Doppler shifted by 1% frequency offset over the PU available bandwidth: (a) Unfiltered PSD; (b) Welch estimated PSD.

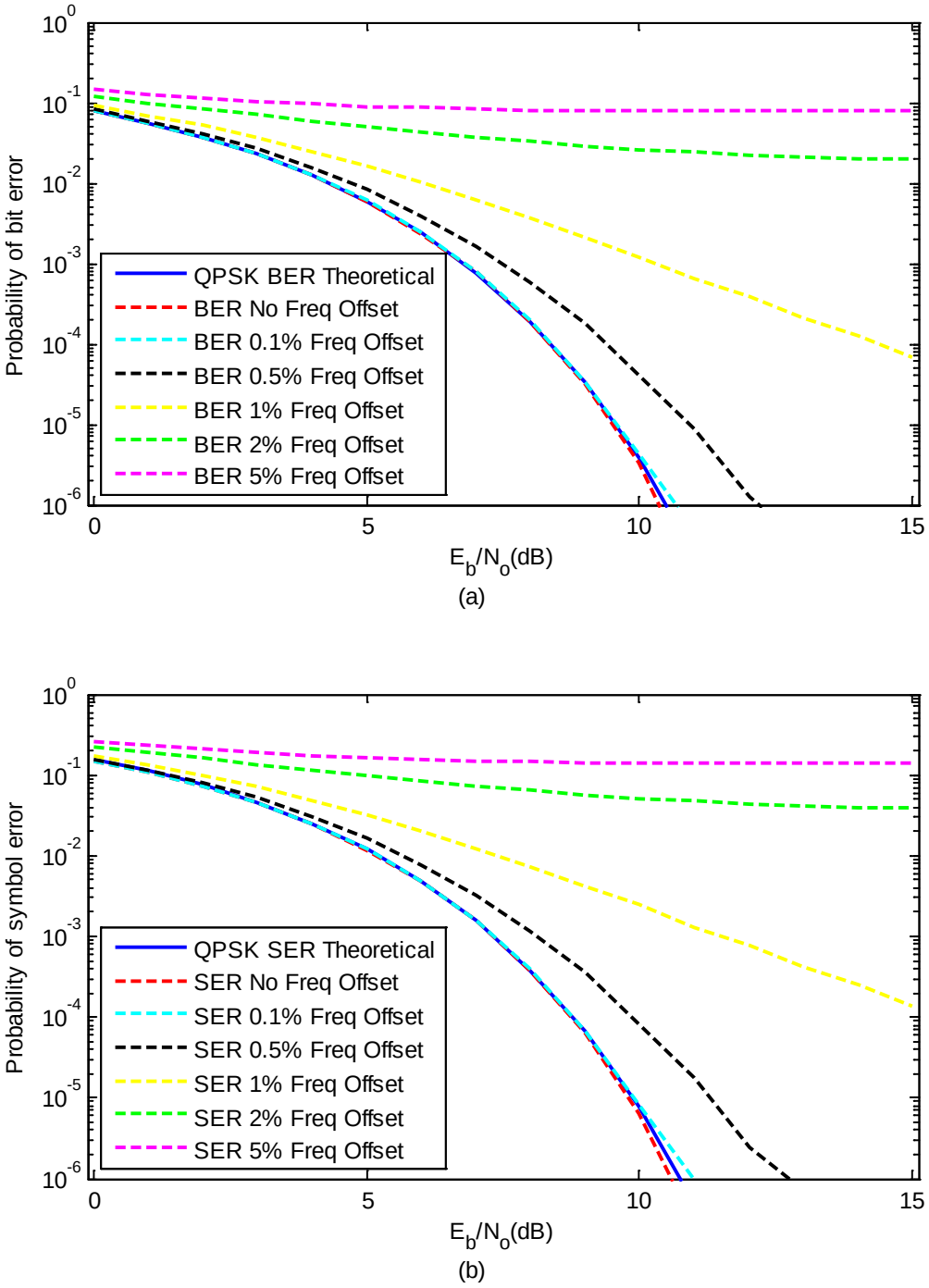

Figure 24. BER performance of PU as a function of Doppler shift on SU where the % frequency offset is the percent over the PU available bandwidth: (a) BER at ***SIR*** = -6 dB; (b) SER at ***SIR*** = -6 dB.

We consider the case when ***SIR*** = -3 dB, which means the sum of the SU signal power is about twice that of the sum of the PU signal power, while we vary the Doppler offset. This is scenario is depicted in Figure 25. In Figure 26, we show the spectra when the SU Doppler offset is 1% of the PU's available bandwidth. Notice the slight frequency shift (as compared to the SU spectrum from Figure 25). This means the subcarriers of the PU and SU added signal are not orthogonal. Since these subcarriers are not orthogonal, the spectral spillage produces errors. The BER and SER for various frequency offsets are shown in Figure 27. We observe that the BER/SER pair resulting from Monte Carlo simulation is not in good agreement with the theoretical BER/SER for QPSK modulation as dictated by Equation (2.2) and (2.4) except without the frequency offset. The BER and SER get worse as the frequency offset gets worse.

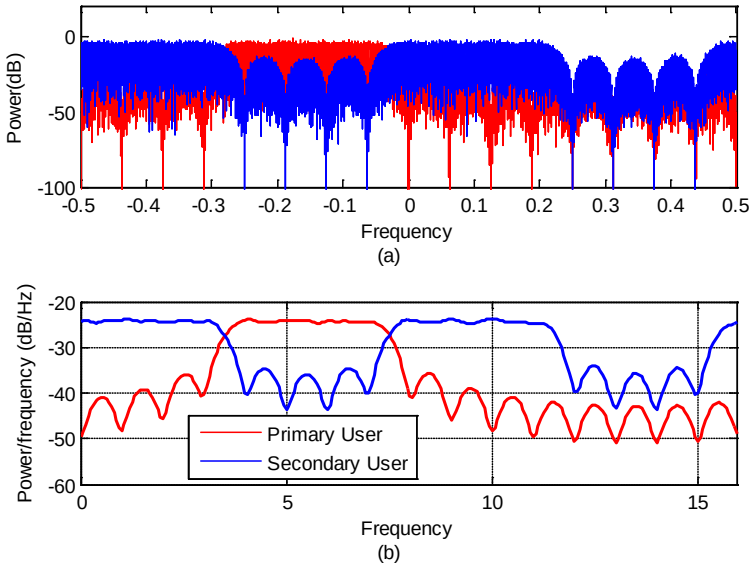

Figure 25. PSDs of PU and SU employing QPSK-OFDM where the PU to SU power ratio is -3 dB (***SIR***): (a) Unfiltered PSD; (b) Welch estimated PSD.

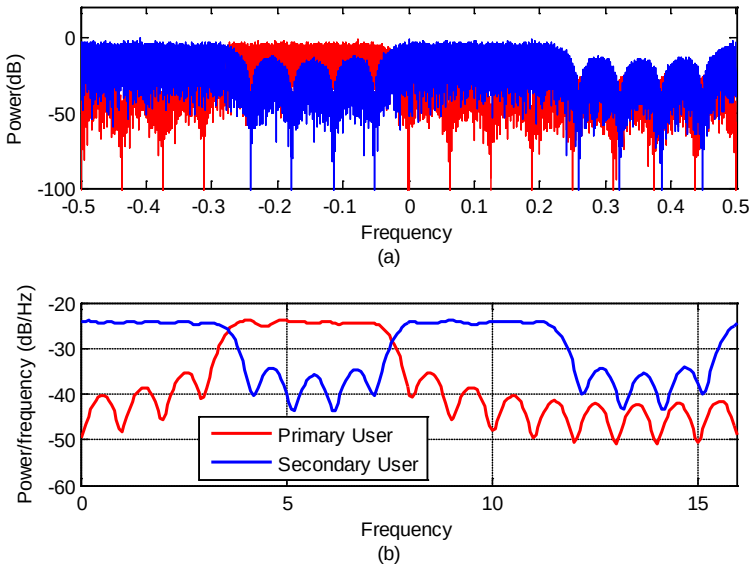

Figure 26. PSDs of PU and SU employing QPSK-OFDM where the PU to SU power ratio is -3 dB (***SIR***) and SU is Doppler shifted by 1% frequency offset over the PU available bandwidth: (a) Unfiltered PSD; (b) Welch estimated PSD.

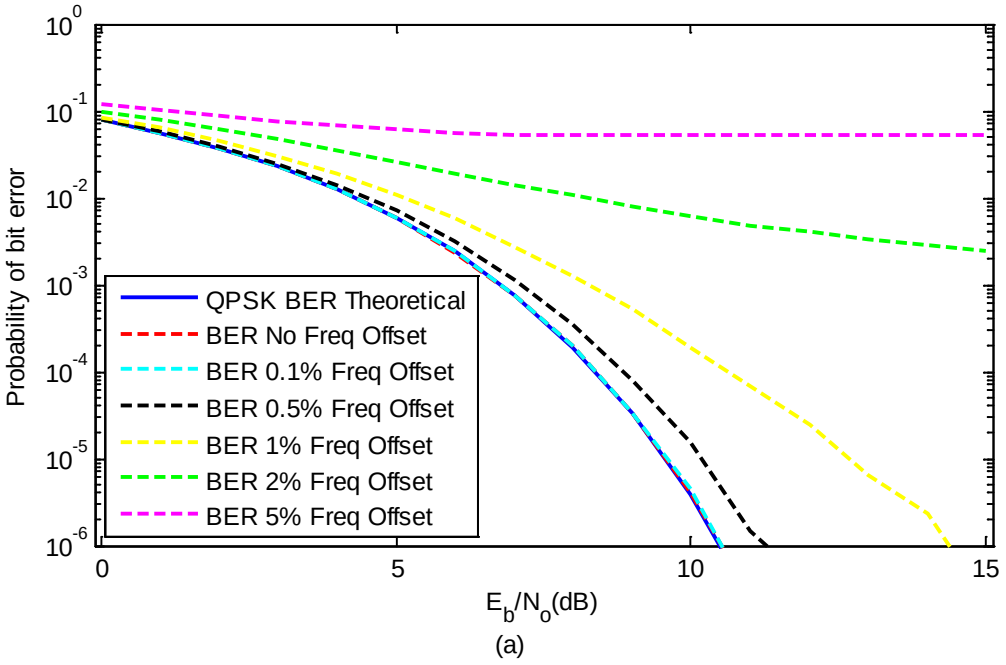

(a)

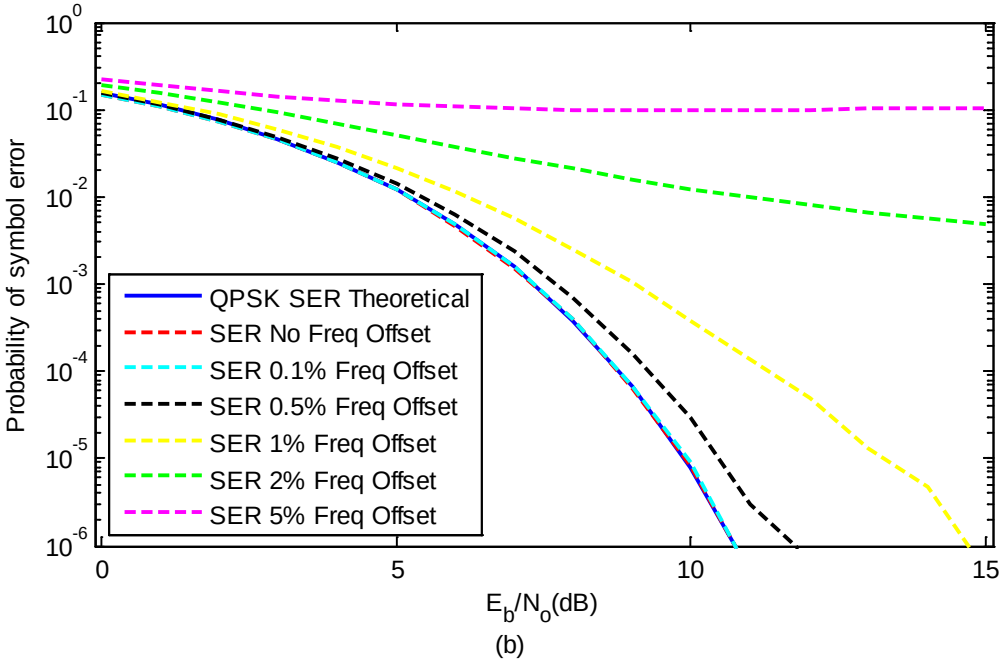

(b)

Figure 27. BER performance of PU as a function of Doppler shift on SU where the % frequency offset is the percent over the PU available bandwidth: (a) BER at ***SIR*** = -3 dB; (b) SER at ***SIR*** = -3 dB.

We consider the case when ***SIR*** = 0 dB, which means the sum of the SU signal power is the same as the sum of the PU signal power while we vary the Doppler offset. This scenario is depicted in Figure 28. In Figure 29, we show the spectra when the SU Doppler offset is 1% of the PU's available bandwidth. Notice the slight frequency shift (as compared to the SU spectrum from Figure 28). This means the subcarriers of the PU and SU added signal are not orthogonal. Since these subcarriers are not orthogonal, the spectral spillage produces errors. The BER and SER for various frequency offsets are shown in Figure 30. We observe that BER/SER pair resulting from Monte Carlo simulation is not in good agreement with the theoretical the BER/SER for QPSK modulation as dictated by Equation (2.2) and (2.4), except without the frequency offset. The BER and SER get worse as the frequency offset gets worse.

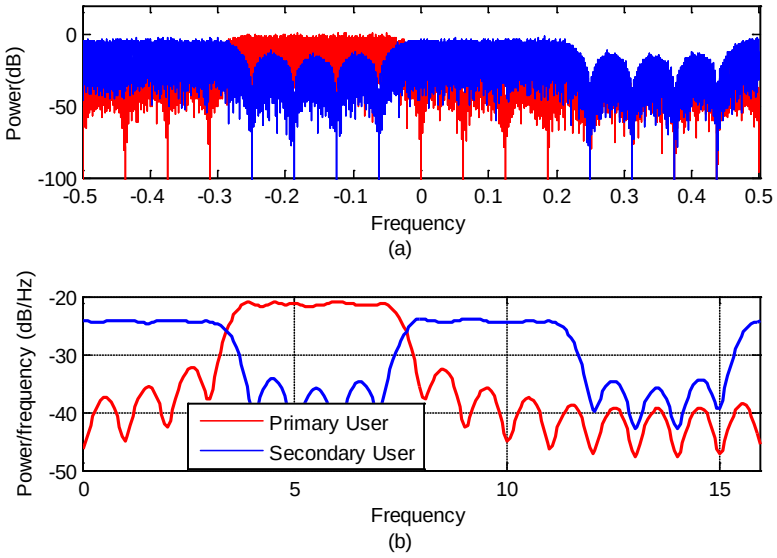

Figure 28. PSDs of PU and SU employing QPSK-OFDM where the PU to SU power ratio is 0 dB (***SIR***): (a) Unfiltered PSD; (b) Welch estimated PSD.

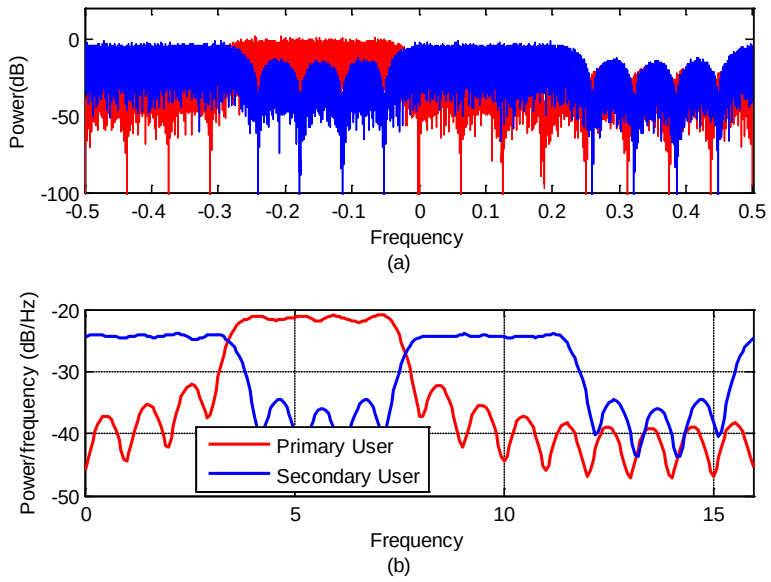

Figure 29. PSDs of PU and SU employing QPSK-OFDM where the PU to SU power ratio is 0 dB (***SIR***) and SU is Doppler shifted by 1% frequency offset over the PU available bandwidth: (a) Unfiltered PSD; (b) Welch estimated PSD.

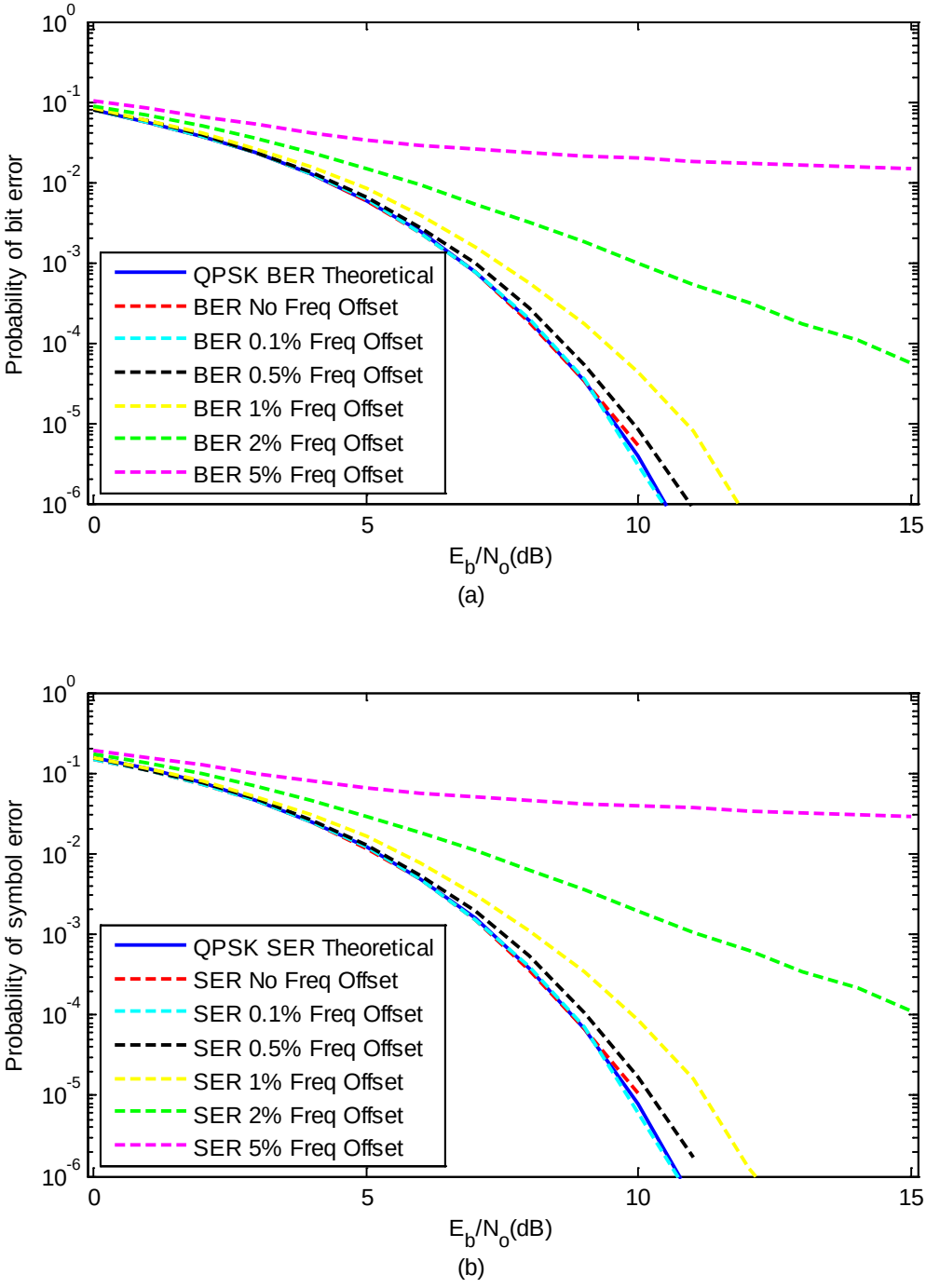

Figure 30. BER performance of PU as a function of Doppler shift on SU where the % frequency offset is the percent over the PU available bandwidth: (a) BER at ***SIR*** = 0 dB; (b) SER at ***SIR*** = 0 dB.

We consider the case when ***SIR*** = 3 dB, which means the sum of the PU signal power is about twice that of the sum of the SU signal power, while we vary the Doppler offset. This scenario is depicted in Figure 31. In Figure 32, we show the spectra when the SU Doppler offset is 1% of the PU's available bandwidth. Notice the slight frequency shift (as compared to the SU spectrum from Figure 31). This means that the subcarriers of the PU and SU added signal are not orthogonal. Since these subcarriers are not orthogonal, the spectral spillage produces errors. The BER and SER for various frequency offsets are shown in Figure 33. We observe that the BER/SER pair resulting from Monte Carlo simulation is not in good agreement with the theoretical BER/SER for QPSK modulation as dictated by Equation (2.2) and (2.4), except without the frequency offset. The BER and SER get worse as the frequency offset gets worse.

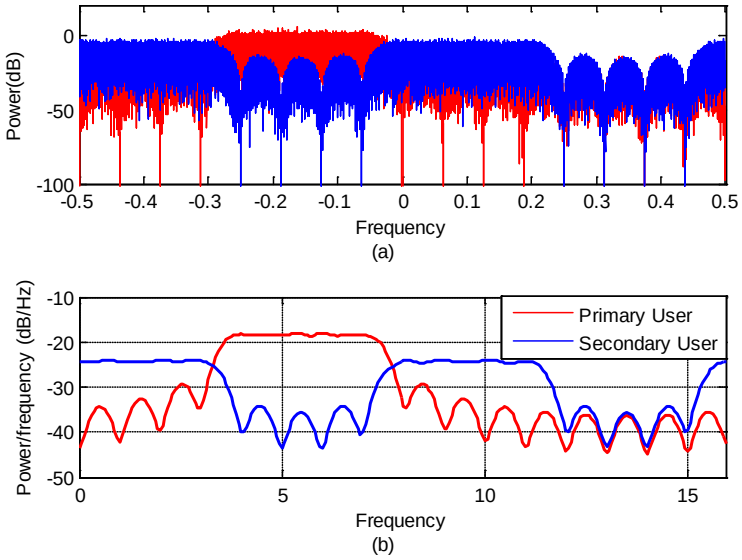

Figure 31. PSDs of PU and SU employing QPSK-OFDM where the PU to SU power ratio is 3 dB (***SIR***): (a) Unfiltered PSD; (b) Welch estimated PSD.

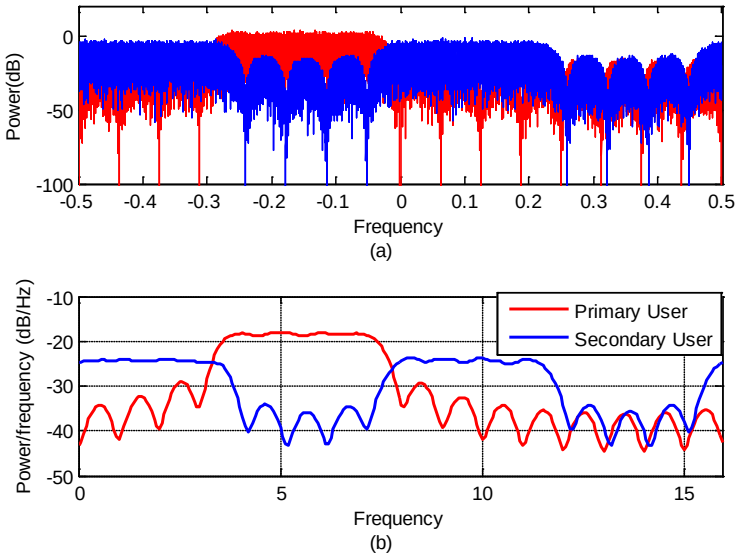

Figure 32. PSDs of PU and SU employing QPSK-OFDM where the PU to SU power ratio is 3 dB (***SIR***) and SU is Doppler shifted by 1% frequency offset over the PU available bandwidth: (a) Unfiltered PSD; (b) Welch estimated PSD.

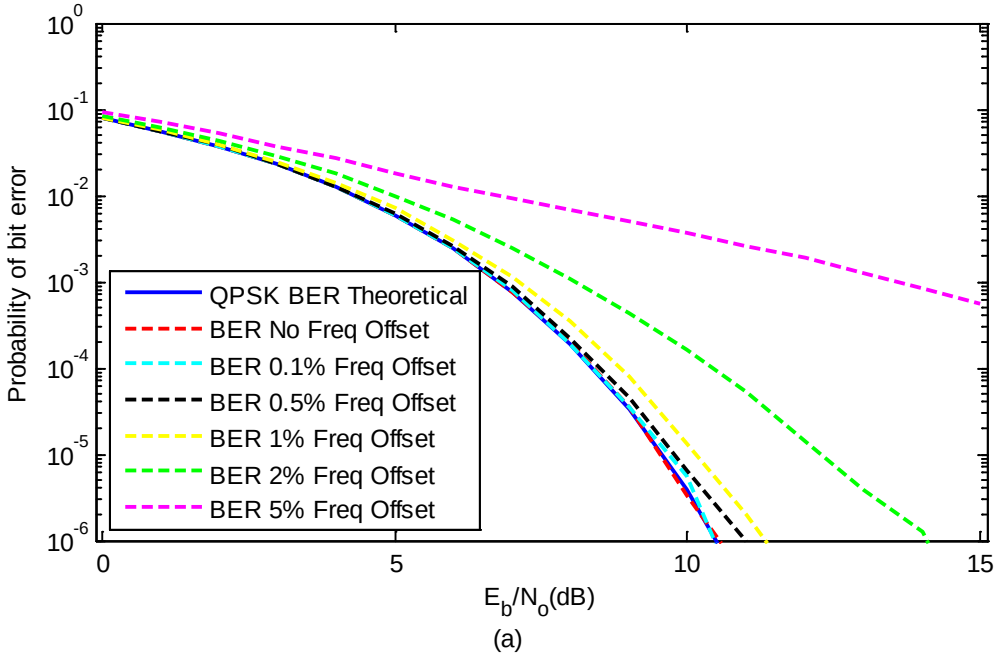

(a)

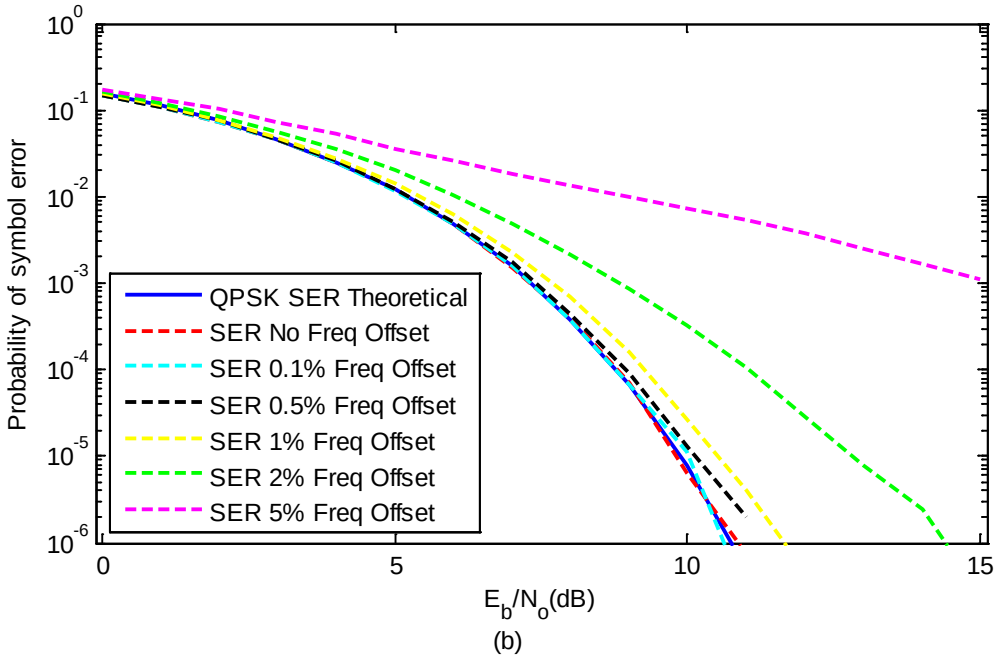

(b)

Figure 33. BER performance of PU as a function of Doppler shift on SU where the % frequency offset is the percent over the PU available bandwidth: (a) BER at ***SIR*** = 3 dB; (b) SER at ***SIR*** = 3 dB.

We consider the case when ***SIR*** = 6 dB, which means the sum of the PU signal power is about four times greater than the sum of the SU signal power, while we vary the Doppler offset. This scenario is depicted in Figure 34. In Figure 35, we show the spectra when the SU Doppler offset is 1% of the PU's available bandwidth. Notice the slight frequency shift (as compared to the SU spectrum from Figure 34). This means that the subcarriers of the PU and SU added signal are not orthogonal. Since these subcarriers are not orthogonal, the spectral spillage produces errors. The BER and SER for various frequency offsets are shown in Figure 36. We observe that the BER/SER pair resulting from Monte Carlo simulation is not in good agreement with the theoretical BER/SER for QPSK modulation as dictated by Equation (2.2) and (2.4), except without the frequency offset. The BER and SER get worse as the frequency offset gets worse.

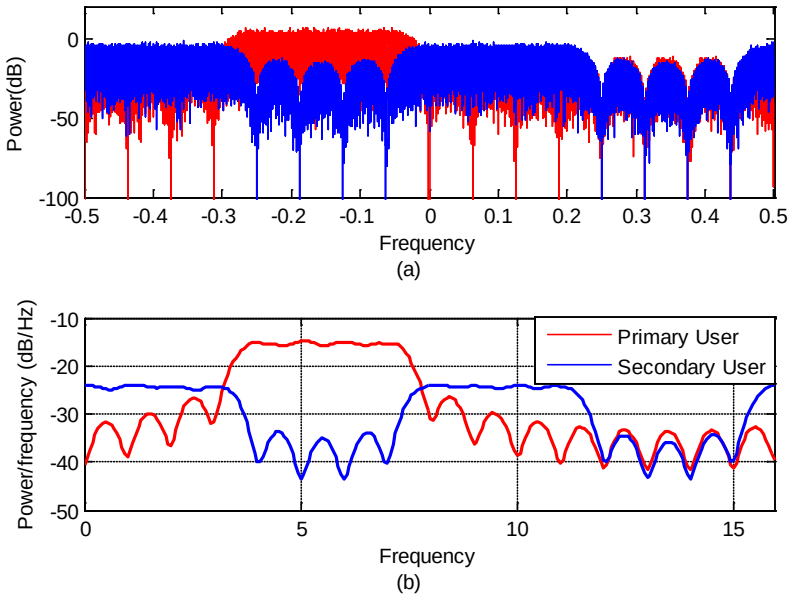

Figure 34. PSDs of PU and SU employing QPSK-OFDM where the PU to SU power ratio is 6 dB (***SIR***): (a) Unfiltered PSD; (b) Welch estimated PSD.

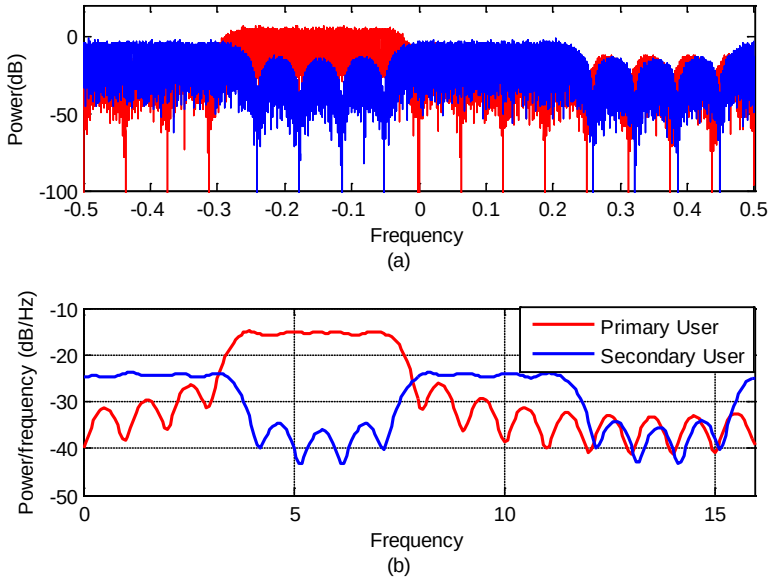

Figure 35. PSDs of PU and SU employing QPSK-OFDM where the PU to SU power ratio is 6 dB (***SIR***) and SU is Doppler shifted by 1% frequency offset over the PU available bandwidth: (a) Unfiltered PSD; (b) Welch estimated PSD.

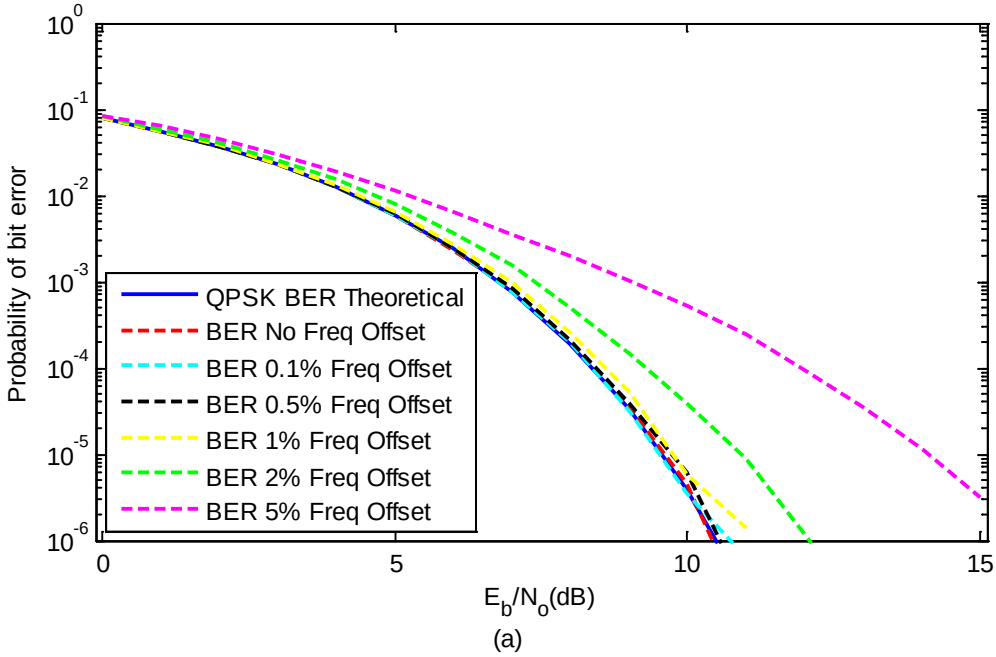

(a)

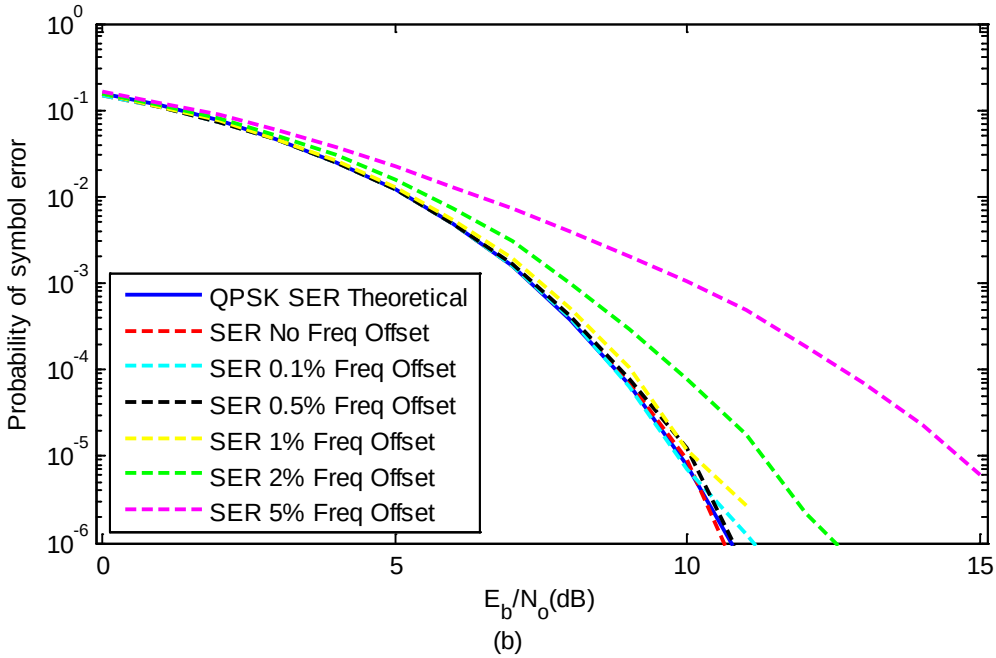

(b)

Figure 36. BER performance of PU as a function of Doppler shift on SU where the % frequency offset is the percent over the PU available bandwidth: (a) BER at ***SIR*** = 6 dB; (b) SER at ***SIR*** = 6 dB.

We consider the case when ***SIR*** = 10 dB, which means the sum of the PU signal power is about 10 times greater than the sum of the SU signal power, while we vary the Doppler offset. This scenario is depicted in Figure 37. In Figure 38, we show the spectra when the SU Doppler offset is 1% of the PU's available bandwidth. Notice the slight frequency shift (as compared to the SU spectrum from Figure 37). This means that the subcarriers of the PU and SU added signal are not orthogonal. Since these subcarriers are not orthogonal, the spectral spillage produces errors. The BER and SER for various frequency offsets are shown in Figure 39. We observe that the BER/SER pair resulting from Monte Carlo simulation is not in good agreement with the theoretical BER/SER for QPSK modulation as dictated by Equation (2.2) and (2.4), except without the frequency offset. The BER and SER get worse as the frequency offset gets worse.

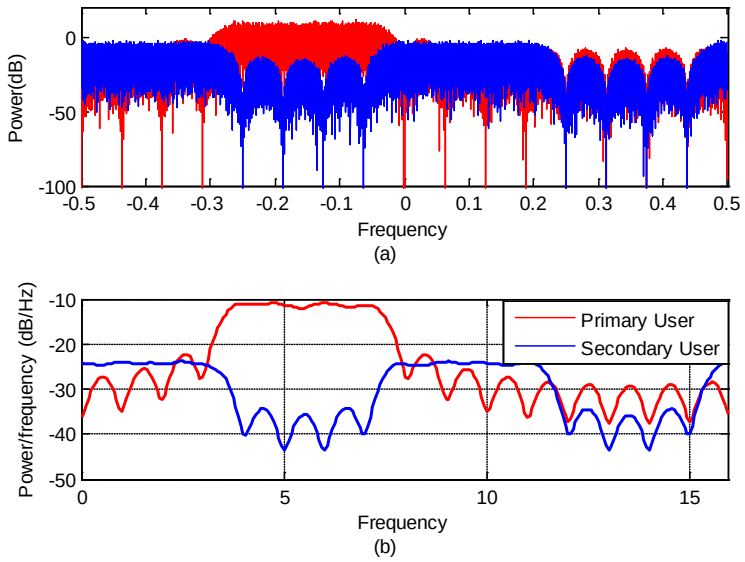

Figure 37. PSDs of PU and SU employing QPSK-OFDM where the PU to SU power ratio is 10 dB (***SIR***): (a) Unfiltered PSD; (b) Welch estimated PSD.

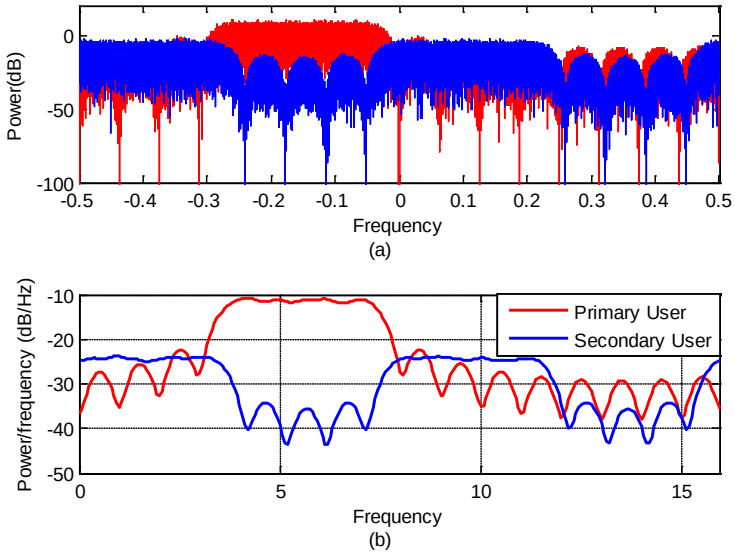

Figure 38. PSDs of PU and SU employing QPSK-OFDM where the PU to SU power ratio is 10 dB (***SIR***) and SU is Doppler shifted by 1% frequency offset over the PU available bandwidth: (a) Unfiltered PSD; (b) Welch estimated PSD.

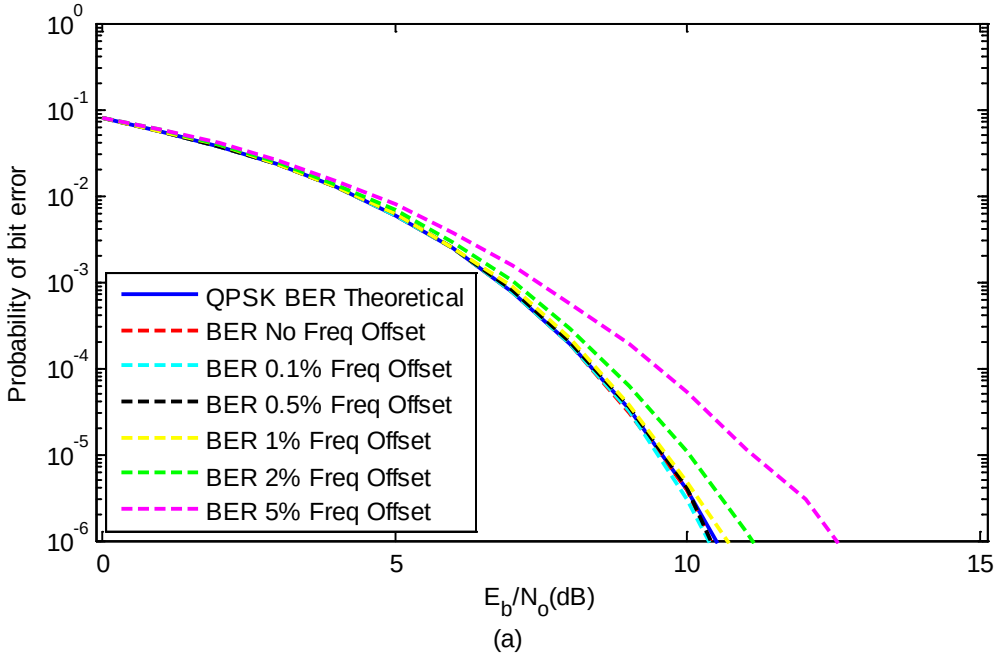

(a)

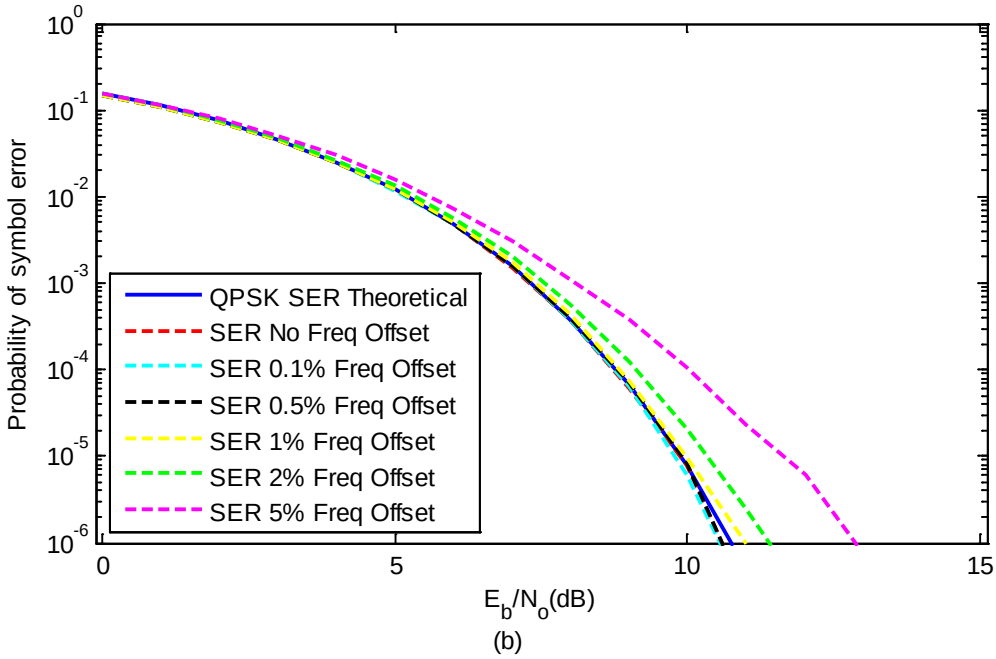

(b)

Figure 39. BER performance of PU as a function of Doppler shift on SU where the % frequency offset is the percent over the PU available bandwidth: (a) BER at ***SIR*** = 10 dB; (b) SER at ***SIR*** = 10 dB.

V. CONCLUSION AND RECOMMENDATIONS

A. CONCLUSION

In this thesis we introduced the notion of adaptive OFDM and how it can be applied to a classic two-user scenario where there is one PU and one SU. Moreover, we investigated the effect on the performance of Doppler shift between PU and SU. With the use of Monte Carlo simulations using Matlab, we were able to show the BER/SER performance curves of OFDM-QPSK and OFDM-16QAM for scenarios where subcarriers are turned off and compare them to theoretical BER/SER expressions as a function of increasing ***SNR***. These scenarios were eight subcarrier (4 ON, 4 OFF), 12 subcarriers (4 ON, 4 OFF, 4 ON), and 16 subcarriers (4 ON, 4 OFF, 4 ON, 4 OFF) with QPSK and 16QAM modulations. The results of these scenarios showed that BER/SER curves of each scenario had good agreement with theoretical BER/SER curves of QPSK or 16QAM.

We also performed simulations of a 12-subcarrier scenario (4 ON, 4 OFF, 4 ON) where we change the power ratio of the two utilized bands while holding total power constant. The result of this simulation showed that the power ratio 1:1 yielded the best performance. The conclusion is that equal power allocation is best for OFDM using the same modulation and an equal number of subcarriers (when two or more bands are available to use).

The last topic we considered was a two-user CR scenario. Two variables in this scenario were the percentage of the SU frequency offset and ***SIR,*** which was changed by adjusting the SU signal power. We set up a 16-subcarrier scenario (4 ON, 4 OFF, 4 ON, 4 OFF) for the PU while the SU utilized the spectrum in this manner (4 OFF, 4 ON, 4 OFF, 4 OFF). With these settings we performed simulations that generated BER and SER by changing ***SIR*** and the percentage of frequency offset. The results showed that without frequency offset, the results showed good agreement with QPSK theoretical BER/SER curves. With frequency offset, as the frequency offset got worse, the BER/SER curves

became worse. When the Doppler shift is fixed, increasing ***SIR*** yields better performance. In other words, increasing ***SIR*** mitigates Doppler effects to a point.

B. RECOMMENDATION FOR THE FUTURE RESEARCH

In this thesis we used the same modulation scheme for the PU and SU. We also used the same number of subcarriers for each channel. In reality, the PU may actually have a different modulation from that of the SU. In adaptive OFDM, each set of subcarriers can use a different modulation and number of subcarriers. Making scenarios more complex, such as using a different number of subcarriers per channel and using different modulations per channel, is a good scenario for future research.

LIST OF REFERENCES

[1] "Spectrum policy task force," Federal Communications Commission, Washington, DC, ET Docket No. 02–135, Tech. Rep., Nov. 2002.

[2] C. Y. Wong, R. S. Cheng, K. B. Letaief, and R. D. Murch, "Multiuser OFDM with adaptive subcarrier, bit, and power allocation," *IEEE J. Sel. Areas Commun.*, vol. 17, no. 10, pp. 1747–1758, Oct. 1999.

[3] G.-R. Lee and J.-H. Wen, "The Performance of Subcarrier Allocation Schemes Combined with Error Control Codings in OFDM Systems," *IEEE Trans. Consumer Electronics.*, vol. 53, no. 3, pp. 852–856, Aug. 2007.

[4] L. Tao, H. M. Wai, V. K. N. Lau, S. Manhung, R. S. Cheng, and R. D. Murch, "Robust joint interference detection and decoding for OFDM based cognitive radio systems with unknown interference," *IEEE J. Sel. Areas Commun*., vol. 25, pp. 566–575, Mar. 2007.

[5] Y. Zhang and C. Leung, "Resource allocation in an OFDM-based cognitive radio system," *IEEE Trans. Commun*., vol. 57, pp.1928–1931, July. 2009.

[6] C. Zhao and K. Kwak, "Power/bit loading in OFDM-based cognitive networks with comprehensive interference considerations: the single-SU case," *IEEE Trans. Veh. Technol*., vol. 59, pp. 1910–1922, Apr. 2010.

[7] M. Morelli and M. Moretti, "Robust frequency synchronization for OFDM-based cognitive radio systems," *IEEE Trans.Wireless Commun*., vol. 7, pp. 5346–5355, Dec. 2008.

[8] C.-H. Hwang, G.-L. Lai, and S.-C. Chen, "Spectrum sensing in wideband OFDM cognitive radios," *IEEE Trans. Signal Process*., vol. 58, pp. 709–719, Feb. 2010.

[9] E. Axell and E. G. Larsson, "Optimal and sub-optimal spectrum sensing of OFDM signals in known and unknown noise variance," *IEEE J. Sel. Areas Commun.*, vol. 29, pp. 290–304, Feb. 2011.

[10] S. Chaudhari, V. Koivunen, and H. V. Poor, "Autocorrelation-based decentralized sequential detection of OFDM signals in cognitive radios," *IEEE Trans. Signal Process.*, vol. 57, pp. 2690–2700, July. 2009.

[11] J. Lund´en, V. Koivunen, A. Huttunen, and H. V. Poor, "Collaborative cyclostationary spectrum sensing for cognitive radio systems," *IEEE Trans. Signal Process.*, vol. 57, pp. 4182–4195, Nov. 2009.

[12] T. T. Ha, "Coherent MPSK," in *Theory and Design of Digital Communication Systems*. New York: Cambridge University Press, pp. 366–371, 2011.

[13] T. T. Ha, “Coherent MQAM and DMQAM,” in *Theory and Design of Digital Communication Systems*. New York: Cambridge University Press, pp. 282–290, 2011.

[14] T. T. Ha, “OFDM,” in *Theory and Design of Digital Communication Systems*. New York: Cambridge University Press, pp. 282–290, 2011.

[15] P. D. Welch, “The Use of Fast Fourier Transform for the Estimation of Power Spectra: A Method Based on Time Averaging Over Short, Modified Periodograms,” *IEEE Trans. Audio Electroacoust.*, vol. AU-15, pp. 70–73, Jun. 1967.

INITIAL DISTRIBUTION LIST

1. Defense Technical Information Center
   Ft. Belvoir, Virginia

2. Dudley Knox Library
   Naval Postgraduate School
   Monterey, California